

MEASUREMENT OF ATMOSPHERIC OPACITY DUE TO WATER VAPOR AT 225 GHz

M. McKinnon

I. Introduction.

The experiment I have performed to fulfill the graduate laboratory requirement for the master's degree in physics is the measurement of atmospheric opacity due to water vapor at 225 GHz. The experiment was supported by the National Radio Astronomy Observatory (NRAO), and was performed under the supervision of Dr. Frazer N. Owen. The experiment used two different designs of radiometers: one designed by NRAO in Tucson, Arizona and the other designed by NRAO's electronics laboratory in Charlottesville, Virginia. The Tucson radiometer was in operation from February 1986 to February 1987. Two radiometers of the Charlottesville design began operations in October 1986 and January 1987. Opacity measurements have been made at NRAO's Very Large Array (VLA) and at the Joint Observatory for Cometary Research (JOCR) on South Baldy mountain. The work I performed in support of this experiment was

1. Automate the operation of the Charlottesville radiometer to perform automatic tipping scans.
2. Revise the method of opacity calculation for the Tucson radiometer, and develop the method of opacity calculation for the Charlottesville radiometer.
3. Perform an error analysis on the data generated by both radiometers.
4. Write various computer programs to display data generated by both radiometers.
5. Design and construct supporting devices to optimize radiometer operation.

II. Charlottesville Radiometer.

A. Operation.

Figure 1 is a schematic diagram of the Charlottesville 225 GHz radiometer. Radiation from the primary mirror (not shown) passes through a four-bladed chopper wheel to the secondary mirror. Radiation from the secondary mirror is focused by a teflon focusing lens into the mixer injection cavity. The signal is mixed with a local oscillator signal in the mixer. The local oscillator is a 75 GHz Gunn diode with a tripler which increases the diode frequency to 225 GHz. The mixed signal is amplified, filtered, attenuated, and then

amplified again before entering the square law detector. The square law detector voltage is synchronized with the chopper wheel in the synchronous detector. The blades of the chopper wheel are angled so that the square law detector alternately senses a hot load (65C), signal, and cold load (45C). The hot and cold loads are thermistors attached to absorber-covered metal plates. The hot and cold loads (not shown in Figure 1) are used to measure the gain of the radiometer (see Section IIB). The radiometer enclosure temperature is maintained at 45C by a thermistor attached to a metal plate inside the radiometer. The radiometer enclosure is insulated on the inside. Inverters maintain a constant voltage at the individual radiometer components by regulating the voltage supplied by the external power supply. The radiometer communicates with a COMPAQ personal computer via an NRAO-designed interface card located inside the radiometer door.

The primary mirror is mounted outside the radiometer enclosure and is driven by a stepping motor. The mirror can rotate 360 degrees by moving 1.8 degrees per step. The mirror beamwidth is approximately 3.4 degrees. An opacity measurement consists of reading the signals from 11 different mirror zenith angles ranging from 7.2 to 70.2 degrees. This range in zenith angle corresponds to a range in airmass of approximately one to three.

The Charlottesville radiometer has a bandwidth of 500 MHz, a two second integration time, a K factor of 1.8, and a 3000K system temperature. Substituting these values into the expression for sensitivity (equation A-8) gives a theoretical sensitivity of 0.2K. With this sensitivity the radiometer can detect fluctuations in signal temperature greater than 0.2K.

There are a number of accessories included with the radiometer which monitor its condition. Temperature sensors monitor the temperatures of the hot load, cold load, ambient air, and enclosure. Ammeters monitor the current of the gunn diode, tripler, mixer, and external power supply. A voltmeter monitors the power supply voltage at the radiometer. A potentiometer attached to the primary mirror shaft measures the mirror zenith angle. A bubble level on the primary mirror mounting plate indicates if the radiometer is level.

B. Data Analysis.

This section discusses how the Charlottesville radiometer data is manipulated to determine scan opacity, zenith opacity, radiometer gain, and atmosphere temperature. The methods used to determine the opacities, gain, and temperature were developed from basic radiometry theory by Dr. Owen and myself.

1. Opacity Calculation.

As shown in Appendix A, the expression for the sky signal temperature is

$$T_s = T_r + T_1(1 - \epsilon) + T_a\epsilon(1 - e^{-A\tau}) + T_{3K}\epsilon e^{-A\tau} \quad (II - 1).$$

where

T_r = receiver temperature
 ϵ = coupling efficiency
 T_1 = temperature at which losses are terminated
 T_a = mean temperature of the atmosphere
 τ = atmospheric opacity
 A = airmass
 T_{3K} = temperature of microwave background radiation.

Since there are no contributions from sources external to the radiometer when it is pointed at a load, the expression for the cold signal temperature is

$$T_{cr} = T_r + T_1(1 - \epsilon) + \epsilon T_c \quad (II - 2)$$

where T_c is 45C. The synchronous detector signal voltage is proportional to the difference in signal temperatures. Taking the difference in cold and sky signal temperatures and denoting the constant of proportionality as g gives

$$\begin{aligned} V_{cs} &= \epsilon g T_c - \epsilon g T_a (1 - e^{-A\tau}) - T_{3K} \epsilon g e^{-A\tau} + V_{do} \\ &= G(T_c - T_a) + G(T_a - T_{3K})e^{-A\tau} + V_{do} \end{aligned} \quad (II - 3)$$

where V_{do} is the synchronous detector offset voltage. The radiometer has been designed such that V_{do} is zero. The product of the coupling efficiency, ϵ , and the constant g is the radiometer internal gain, G . The contribution due to background radiation, T_{3K} , may be neglected since it is approximately one percent of the atmosphere temperature, T_a . Rearranging equation II - 3 and taking its natural logarithm gives

$$\ln(V_{cs} - G(T_c - T_a)) = \ln(GT_a) - A\tau \quad (II - 4).$$

Equation II - 4 is the equation of a straight line with a negative slope equal to the opacity in magnitude. Since the radiometer can take readings at different elevations (airmasses), the opacity may be calculated by applying a linear least squares analysis to the radiometer data using equation II - 4. Methods for determining the atmosphere temperature and radiometer gain are discussed later in this report. A sample of the data generated by this method is shown in Figure 2.

The atmospheric opacity at zenith may be determined independently of the scan opacity discussed above. The zenith opacity is a single point measurement of the opacity at an airmass equal to one. The signal voltage at zenith is

$$V_{cs} = G(T_c - T_a) + GT_a e^{-\tau} \quad (II - 5).$$

Rearranging equation II - 5 and taking its natural logarithm gives

$$\tau = -\ln(V_{cs}/G + (T_a - T_c)/T_a) \quad (II - 6).$$

During a measurement, the computer controlling the radiometer can calculate both a scan opacity and a zenith opacity. These are essentially two independent measurements of

the same thing. A comparison of the two opacities is an indication of how well one may believe the measurements. A comparison of the two measurements is shown in Figure 3. Note the appearance of more scatter in the zenith opacities than in the scan opacities. The scan opacity varies less than the zenith opacity because the scan opacity is a multiple point measurement whereas the zenith opacity is a single point measurement.

The scan opacity may be calculated by another method I developed which makes no assumptions about detector offset voltage, atmosphere temperature, or gain correction. The method allows one to calculate the gain and atmosphere temperature in addition to the opacity. The method, discussed in Appendix C, uses a Taylor's expansion about zero airmass, and is less stable than the linear technique.

2. Gain Calculation.

The internal gain of the radiometer can be determined using the signals from the hot and cold loads. Since there are no contributions from sources external to the radiometer when it is pointed at a load, the expressions for the hot signal temperature and cold signal temperature become

$$T_{hr} = T_r + T_1(1 - \epsilon) + \epsilon T_h \quad (II - 7)$$

$$T_{cr} = T_r + T_1(1 - \epsilon) + \epsilon T_c \quad (II - 8)$$

respectively, where T_h is 65C and T_c is 45C. The synchronous detector voltage is proportional to the difference in hot signal temperature and cold signal temperature.

$$V_{hc} = G(T_h - T_c) + V_{do} \quad (II - 9)$$

The internal gain may be computed directly since the detector voltages and temperatures are known and V_{do} is zero. This particular design feature of the radiometer can be used to correct radiometer data for variations in internal gain.

The internal gain is designated as "internal" because it is the gain determined within the radiometer. Other contributions external to the radiometer may cause the external gain to differ from the internal gain. The external gain is determined by placing two loads with different temperatures in the mirror beam and observing the radiometer signal response. The external gain must be used in the opacity calculations. The program which controls the radiometer, CVTIPPER, does this by applying a correction factor to the internal gain. The correction factor is assumed to be constant with time, and is determined by equating zenith opacity to scan opacity.

3. Determination of Atmosphere Temperature.

As seen in equation II - 6, an estimate of the atmosphere temperature must be made before the opacity can be calculated. The atmosphere temperature is assumed to follow an

adiabatic lapse rate weighted by the exponential distribution of water vapor. The adiabatic lapse rate is the deviation with height of the atmosphere temperature from the ambient ground temperature. Therefore the average atmosphere temperature is

$$T_a = T_{amb} - \frac{\int_0^{\infty} L h e^{h/h_o} dh}{\int_0^{\infty} e^{h/h_o} dh} \quad (II - 10)$$

where

- T_{amb} = ambient temperature
- L = adiabatic lapse rate
- h = elevation above site
- h_o = scale height.

Performing the integration gives

$$T_a = T_{amb} - L h_o \quad (II - 11).$$

Assuming an adiabatic lapse rate of 9.8K per kilometer and a scale height of 1.8 kilometers gives an atmosphere temperature which is 17K below ambient temperature. Since the Charlottesville radiometer monitors the ambient temperature, the atmosphere temperature can be calculated.

Another method of determining the temperature of the atmosphere is discussed in Section III, namely, the atmosphere temperature is 95 percent of the ambient temperature. The Section III method was the first attempt at estimating the atmosphere temperature, and is strictly empirical. It was decided that the lapse rate method was a more accurate estimate of the atmosphere temperature.

III. Tucson Radiometer.

A. Operation.

Figures 4A and 4B are schematic diagrams of the Tucson 225 GHz radiometer local oscillator circuit and detector circuit. Radiation from the primary mirror passes through a two-bladed chopper wheel to the secondary mirror. Radiation from the secondary mirror passes through a polarizing grid before entering the mixer. The local oscillator is a 75 GHz gunn diode. The local oscillator radiation passes through an isolator, directional coupler, variable attenuator, and tripler before entering the polarization grid. The isolator prevents the backflow of radiation power. The directional coupler splits the local oscillator radiation. Ten percent of the radiation entering the directional coupler is available at a power meter connection and the remaining 90 percent passes on to the variable attenuator.

The variable attenuator adjusts the radiation power to an acceptable level for the tripler. The tripler increases the diode frequency to 225 GHz.

After passing through the polarizing grid, the signal radiation is mixed with the local oscillator radiation. The mixed signal passes through an arrangement of amplifiers, attenuators, and filters before entering the detector. The detector measures the incoming signal and synchronizes it with the chopper wheel. The chopper is located at the focus of the primary mirror. The chopper wheel blades are flat, and are covered with absorber material on the side facing the secondary mirror. The temperature of the chopper wheel blades is assumed to be ambient temperature.

The primary mirror is located inside the radiometer enclosure, centered on a transparent window. The mirror beamwidth is also about 3.4 degrees. The opacity is measured similarly to the Charlottesville radiometer, except the mirror zenith angle ranges from 7.2 to 76.0 degrees. This range in zenith corresponds to a range in airmass of about one to four. The theoretical sensitivity of the Tucson radiometer is similar to the sensitivity of the Charlottesville radiometer.

B. Data Analysis.

This section describes how I revised the Tucson radiometer opacity calculation method. The original method assumed that the ambient temperature and atmosphere temperature were equal. Using the expression for signal temperature from Appendix A, the respective expressions for the sky signal temperature and reference temperature are

$$T_s = T_r + T_1(1 - \epsilon) + T_{amb}\epsilon(1 - e^{-A\tau}) + T_{3K}\epsilon e^{-A\tau} \quad (III - 1)$$

$$T_{ref} = T_r + T_1(1 - \epsilon) + \epsilon T_{amb} \quad (III - 2).$$

where T_{amb} is the ambient temperature. Taking the difference in reference and sky signal temperatures, neglecting contributions from background radiation, and multiplying by the gain gives

$$V_{rs} = \epsilon g T_{amb} e^{-A\tau} + V_{do} \quad (III - 3).$$

V_{do} for the Tucson radiometer is not zero. The Tucson radiometer was designed so that its detector offset voltage could be measured. Rearranging equation III - 3 and taking its natural logarithm gives

$$\ln(V_{rs} - V_{do}) = \ln(GT_{amb}) - A\tau \quad (III - 4).$$

Equation III - 4 is the equation of a straight line with a negative slope equal to the opacity in magnitude. The opacity is calculated by applying a linear least squares analysis to the radiometer data with the program BIGGRAPH.PAS. A sample of this method is shown graphically in Figure 5. The straight line generated by this method usually did not represent the data. As can be seen in Figure 6, the data is more accurately represented

by a quadratic. The quadratic was generated by noting that ambient temperature and atmosphere temperature are not the same. Equation III - 4 should then be changed to

$$\ln(V_{rs} - V_{do}) = \ln(G) + \ln((T_{amb} - T_a) + T_a e^{-A\tau}) \quad (III - 5).$$

Performing a Taylor's expansion about zero airmass on the second term in the right-hand side of equation III - 5 changes the equation to

$$\ln(V_{rs} - V_{do}) = \ln(GT_{amb}) - \tau AT_a/T_{amb} + ((T_a T_{amb} - T_a^2)\tau A/T_{amb})^2/2 \quad (III - 6).$$

The opacity in this case is determined with a quadratic least squares analysis performed by the program POLYFIT.PAS. The polynomial method effectively demonstrated that the ambient temperature and atmosphere temperature are not the same; however, the method is only a second order approximation. We consulted personnel at NRAO's 12-meter telescope at Kitt Peak and found that the atmosphere temperature is about 95 percent of ambient temperature at 225 GHz. Inserting this result into equation III - 5 and rearranging gives

$$\ln(V_{rs} - V_{do}) - (0.05GT_{amb}) = \ln(0.95GT_{amb}) - A\tau \quad (III - 7).$$

Equation III - 7 is also the equation of a straight line with a slope equal to the opacity. The opacity can be determined by performing a linear least squares analysis on the radiometer data with the ambient temperature as a variable. This calculation is performed in the program CONSTANT.PAS. The graph generated by CONSTANT is shown in Figure 7. Although the Tucson radiometer does not monitor ambient temperature, the temperature is monitored at a VLA weather station.

IV. Sources of Error.

Since operation of the Tucson radiometer had already started before I became involved with this project, most of my efforts in reducing sources of error were directed towards the Charlottesville radiometer. However, the propagation of errors in the data sets of both radiometers is similar, and the detailed error analysis calculations appear in Appendix B. The calculations determine the error bars associated with the data points plotted in the figures displayed in this report. The calculations also determine the error in calculated opacity.

Possible sources of error in the Charlottesville radiometer can be attributed to

1. Not allowing enough time for the primary mirror to move to its new elevation.
2. Not allowing enough integration times before recording data at each elevation.
3. Direct sunlight impinging upon the primary mirror.
4. Indirect sunlight reflected from surfaces onto the primary mirror.

5. Obstacles such as people, vehicles, and the Sun in the mirror beam.
6. Approximating the airmass as strictly the secant of the zenith angle.
7. Scanning the atmosphere over too large a range in airmass.
8. Ice on the primary mirror.

It was obvious that not enough time was allowed for the primary mirror to move because the radiometer would not respond to commands from the computer. This difficulty was overcome by simply executing a 100 millisecond time delay before the mirror was stepped again.

Once the computer and radiometer were communicating, it was noted that the rms at low airmasses was much higher than the rms at high airmasses (20 millivolts as compared to 0.3 millivolts). The primary mirror must move through a larger change in elevation at low airmasses than at high airmasses for the same change in airmass. As a result, the change in signal between consecutive airmasses is greater at low airmasses than at high airmasses. Since the radiometer integration time is two seconds, the device could not respond fast enough for the large change in elevation. The rms was reduced to about 0.3 millivolts at all airmasses by inserting a 10 second time delay (five integration times) before the computer began collecting data.

The signal rms was further reduced by noting that sunlight and reflections altered the signal. An enclosure was built to shield the radiometer from the sun, reflections, and wind. A window was left in the enclosure so the mirror beam would not "see" the enclosure. The contribution to error due to obstacles was eliminated by installing the radiometers in low pedestrian and vehicle traffic areas.

Data from the Tucson radiometer was used to investigate the effect of different airmass estimates upon calculated opacity. Airmass is approximated as the secant of the zenith angle. A more accurate estimate of the airmass is given by

$$A = \sec(z) - 0.0018167(\sec(z) - 1) - 0.002875(\sec(z) - 1)^2 - 0.0008083(\sec(z) - 1)^3 \quad (V - 1)$$

where z is the zenith angle. I wrote the program SECANT.PAS to plot Tucson radiometer data versus airmass as calculated by equation $V - 1$. The results of SECANT.PAS were compared with those of BIGGRAPH.PAS, which approximated airmass as the secant of the zenith angle. As can be seen from Figures 8A and 8B, the calculated opacity does not differ significantly between airmass calculation methods. We decided to use the secant approximation to reduce computer calculation time.

Data from the Tucson radiometer also indicated that we were scanning over too large a range in airmass. The error in airmass at about four airmasses is greater than that at three airmasses. This is evident in Figure 7. The scan was changed from 11 data points over a range of three airmasses to 11 data points over a range of two airmasses.

Ice on the primary mirror of the Charlottesville radiometer scatters radiation. This produces a high rms in the detected signal. The ice is a problem only when temperatures at the radiometer location cycle about the freezing point of water. The ice does not form if the temperature is constantly above or below freezing. We are in the process of designing a computer-actuated heating system to melt the ice which accumulates on the mirror.

V. Software.

I have written numerous programs to control the radiometer and display the data generated by it. This section will briefly describe the software used with the radiometers. Copies of these programs are in Appendix D.

CVTIPPER.COM is a program I consolidated that controls the Charlottesville radiometer and calculates opacities. The basic sequence of commands in CVTIPPER is

1. Create data file
2. Create monitor file
3. Establish communications with radiometer
4. Move primary mirror to zenith
5. Save monitor data in monitor file
6. Calculate zenith opacity
7. Execute tipping scan
8. Display scan data
9. Calculate scan opacity
10. Save scan data in data file.

CVTIPPER writes opacity data to a data file every 10 minutes and monitor data to a monitor file every 30 minutes. New monitor files and data files are created each day. The data stored in the data file includes the date and time the scan was executed, the scan opacity and its error, the equivalent airmass at each elevation, and the rms in signal voltage at each elevation. The information in the monitor file includes all the temperatures, currents, and voltages monitored by the radiometer. Those points monitored are

1. Signal-cold reference temperature
2. Hot-cold reference temperature
3. System temperature
4. Cold reference temperature
5. Hot reference temperature
6. Ambient temperature
7. Enclosure temperature
8. Mixer current
9. Tripler current
10. Gunn current
11. Supply voltage at radiometer
12. Zenith angle
13. Supply current
14. Spare
15. Spare
16. Spare

The monitor points are stored so that component historical performance can be accessed in the event of a hardware malfunction. The displays of CVTIPPER during and after a tipping scan are shown in Figures 9A and 9B, respectively.

SKY.PAS and DATGRAPH.PAS are programs I wrote which graph opacity as a function of time. SKY accesses the data files created by CVTIPPER for the date, times, scan opacity, and zenith opacity. SKY then plots both opacities for all times stored in the data file. SKY gives the user the option of selecting three vertical scales depending upon the maximum opacity in the file to be graphed. These maximum opacities are 0.25, 0.50, and 1.0. The display of SKY is shown in Figure 3. DATGRAPH is similar to SKY except it plots opacity data from the Tucson radiometer. The display of DATGRAPH is shown in Figure 10.

CVADJUST.PAS, SECANT.PAS, CONSTANT.PAS, and POLYFIT.PAS are all variations of the program BIGGRAPH.PAS which graphs the data from each opacity scan. CVADJUST is the only program used with the Charlottesville radiometer data. All of these programs use raw data from the data file to recalculate the scan opacity and calculate the errors associated with each data point. The programs then plot the logarithm of detector voltage versus airmass with error bars, except CVADJUST and CONSTANT which plot the logarithm of corrected detector voltage as discussed in sections IIB and IIIB. The error bars are usually much smaller than the symbol used to represent the data point. The displays of CVADJUST, SECANT, CONSTANT, POLYFIT, and BIGGRAPH are shown in Figures 2, 8B, 7, 6, and 8A, respectively.

TEMPGRAF.PAS is a program I wrote which plots Charlottesville radiometer enclosure temperature and ambient temperature versus time. TEMPGRAF accesses the monitor file for the temperatures and times. TEMPGRAF is used to observe the response of the radiometer temperature controller to variations in ambient temperature. The display of TEMPGRAF is shown in Figure 11.

VI. Periphereal Devices.

The installation of the radiometer on South Baldy required the design and construction of a support stand and an enclosure. The support stand was orginally designed to support the Tucson radiometer, but was later modified to support the Charlottesville radiometer and its enclosure. The enclosure was built to shield the radiometer from the weather as described in Section IV. The design drawings I produced for the stand and enclosure are shown in Figures 12A, 12B, 12C, and 12D, respectively.

When the COMPAQ personal computer which controls the radiometer is turned off, it cannot be restarted for another twenty seconds. Supposedly, a capacitor built into the computer must discharge before the computer will reboot. This protects the computer from power surges during a power dip. An undesirable result of this design feature is that the computer will not reboot if power is restored within twenty seconds. If a power dip occurred, we wanted the computer to reboot automatically since it was located at a remote site. We were able to automatically reboot the computer by installing a time delay

relay in the computer power supply line. The time delay relay is set for a time longer than twenty seconds so the capacitor in the computer can discharge. The circuit I designed for the time delay relay is shown in Figure 13.

Measures were also taken to improve the telephone line at JOCR since we hope to transfer radiometer data via a modem. The original telephone line was unprotected and laid above ground. A new telephone line was pulled through a new buried conduit. I modified a junction box so that an above ground multiconductor cable could be terminated and tied to the new telephone line. The drawings for the junction box modification, junction box foundation, and terminal strip installation are shown in Figures 14A, 14B, and 14C, respectively.

VII. Conclusions.

Data from the radiometers are consolidated and plotted on graphs as shown in Figures 15 and 16. Each figure displays a consistent minimum opacity. The minimum opacity at South Baldy is about 0.03 while the minimum opacity at the VLA is about 0.10. The opacity at South Baldy is consistently less than the opacity at the VLA by at least a factor of two. Sometimes this opacity ratio may be as high as four. The opacity at either site is the smallest during the winter months of December through March. The opacity is especially low immediately following the passing of a weather front.

No consistent pattern of opacity fluctuation is observed on a daily basis. The opacity is extremely random on stormy winter days, but is constant on clear winter days. Some night-day variations may be present at the VLA during summer months as shown in Figure 10. I have interpreted this figure as water vapor being driven into the atmosphere as the sun rises, with the opacity reaching a maximum in the afternoon. As the sun sets, the atmosphere cools and the water vapor condenses, decreasing the atmospheric opacity.

APPENDIX A : Radiometry Theory.

1. Radiative Transfer.

The radiative transfer equation for a constant source function, S , is

$$I = I_o e^{-d} + S(1 - e^{-d}) \quad (A - 1)$$

where

I = observed brightness

I_o = background source brightness

d = optical depth.

A medium is optically thick if $d > 1$, and is considered optically thin if $d < 1$. An optically thick medium is one in which a photon of frequency ν is absorbed before it can traverse the medium. An optically thin medium is one in which the photon traverses the medium before it is absorbed.

For blackbody radiation the brightness can be described by Planck's Law

$$I = B = \frac{2h\nu^3}{c^2 e^{(h\nu/kT)} - 1} \quad (A - 2).$$

In the Rayleigh-Jeans region of the blackbody spectrum ($h\nu \ll kT$), the brightness may be further simplified to

$$B = 2\nu^2 kT/c^2 \quad (A - 3)$$

Substituting equation A - 3 into equation A - 1 gives

$$T_b = T_{bo} e^{-d} + T(1 - e^{-d}) \quad (A - 4).$$

The Rayleigh-Jeans approximation can be made in the case of the 225 GHz radiometers since the atmosphere temperature is about 265K. One may calculate $h\nu/kT$ and find that it is 0.04, which is much smaller than one.

Equation A - 4 does not accurately represent the temperature detected by a radiometer. The inefficiency in coupling the radiometer antenna to its receiver causes the incoming signal to be attenuated. The attenuation is also a source of noise power in the radiometer. The inefficiency is accounted for by a coupling efficiency denoted by ϵ . Therefore all temperatures detected by the radiometer are reduced by the coupling efficiency, and the noise contribution is $T_1(1 - \epsilon)$, where T_1 is the temperature at which losses are terminated. T_1 may be thought of as the physical temperature of the antenna (ambient), but this is an insignificant point since radiometers are designed to eliminate T_1 .

Also, all the aforementioned temperatures are relative to the radiometer system temperature. All of the radiometer components have a noise power associated with them. By

Nyquist's theorem, the noise power of a component can be represented by a component temperature. The system temperature represents the contributions of all components. Note that the system temperature is not attenuated by coupling efficiency.

The actual temperature detected by the radiometer is the sum of system temperature, attenuated noise temperature, and equation A-4 corrected for coupling efficiency.

$$T_s = T_r + T_1(1 - \epsilon) + T_a \epsilon(1 - e^{-d}) + T_{3K} \epsilon e^{-d} \quad (A - 5)$$

where

T_s = signal temperature

T_r = system temperature

T_a = atmosphere temperature

T_{3K} = background radiation temperature

The third term in equation A - 5 is the contribution of the source being observed (atmosphere), and the last term is the attenuation of the background radiation by the source.

2. Opacity.

The optical depth, d , is the product of the opacity at zenith, τ , and the airmass, A .

$$d = \tau A \quad (A - 6)$$

The opacity at 225 GHz is due to water vapor and oxygen. The opacity due to oxygen is essentially constant at about 0.005 nepers. The opacity due to water vapor is proportional to the amount of precipitable water vapor in the atmosphere.

$$\tau = \beta(225)W \quad (A - 7)$$

where $\beta(225)$ is the constant of proportionality (nepers/mm) and W is the amount of water vapor (mm). Although the proportionality constant is a function of elevation, it is approximately constant at 0.06 neper/mm. Therefore a measurement of the opacity will allow one to calculate the amount of precipitable water vapor in the atmosphere.

3. Sensitivity.

The sensitivity of a radiometer is the smallest change in system input which can be detected by the radiometer. It is the limitation of radiometer performance. Sensitivity is given by the expression

$$\Delta T = KT_r / \sqrt{Bt} \quad (A - 8).$$

where

B = radiometer bandwidth

t = radiometer integration time

T_r = radiometer system temperature

K = factor determined by type of radiometer.

APPENDIX B : Error Analysis.

1. Error Bars.

The vertical error bars in the plots of the natural logarithm of detector voltage versus airmass are determined by the root mean square (rms) of detector voltage. The rms (standard deviation) is calculated with the equation

$$\sigma^2 = \sum (x_i - \mu)^2 / N \quad (B - 1)$$

where

σ = rms

N = number of measurements

x_i = i th measurement of the detector voltage

μ = mean detector voltage.

The upper limit on detector voltage in a plot is the natural logarithm of the sum of mean detector voltage (or corrected detector mean detector voltage depending upon the program) and rms. The lower limit is the natural logarithm of the difference in mean detector voltage and rms. The graphics programs draw the vertical error bars by drawing a line through the points determined by the upper and lower limits.

The horizontal error bars are determined by the error in the secant of the zenith angle. The error in $\sec(z)$ is just the absolute value of the derivative of $\sec(z)$ with respect to z .

$$d(\sec(z)) = | -\tan(z)\sec(z)dz | \quad (B - 2)$$

The error, dz , in zenith angle is assumed to be one degree. The upper limit in airmass is the sum of the airmass and $d(\sec(z))$. The lower limit in airmass is the difference between airmass and $d(\sec(z))$. The graphics programs draw horizontal error bars by drawing a line through the points determined by the upper and lower limits of airmass.

2. Weighting.

As stated in Section IV, the error associated with a measurement at high airmass is greater than the error at low airmass. This implies that the calculated opacity should be weighted towards data points taken at low airmass. The general equation for the slope of a straight line in least squares analysis is

$$m = \frac{\sum x_i y_i - \sum x_i \sum y_i / N}{\sum x_i^2 - (\sum x_i)^2 / N} \quad (B - 3)$$

where

m = slope of the line
 y_i = ordinate coordinate
 x_i = abscissa coordinate
 N = number of data points.

The general equation for the slope of a straight line in a weighted least squares analysis is

$$m = \frac{\sum x_i y_i \sum w_i - \sum x_i \sum y_i}{\sum x_i^2 \sum w_i - (\sum x_i)^2} \quad (B - 4)$$

where w_i is the weighting factor for each data point. In the opacity calculation, y_i is the natural logarithm of corrected detector voltage, x_i is the airmass, and m is the opacity. From Bevington, the weighting factor for an exponential function is the exponent of y_i , which is just the corrected detector voltage in this case.

3. Error in Calculated Opacity.

The uncertainty in the calculated opacity depends upon how well the data points are described by a straight line. Given the equation of a straight line, $y = mx + a$, the uncertainty in the calculated slope (m) of a line in least squares analysis is approximately

$$\sigma_m^2 = N\sigma_s^2/\delta \quad (B - 5)$$

where

$$\sigma_s^2 = \sum (y_i - a - mx_i)^2 / (N - 2) \quad (B - 6)$$

$$\delta = N \sum x_i^2 - (\sum x_i)^2 \quad (B - 7)$$

and N is the number of data points.

If the data are weighted, as in the case under consideration, the uncertainty in the slope is

$$\sigma_m^2 = (\sum w_i)\sigma_s^2/\delta_w \quad (B - 8)$$

where

$$\delta_w = \sum w_i \sum x_i^2 - (\sum x_i)^2 \quad (B - 9)$$

and N and σ_s are as previously defined. Recall that in the opacity calculation, y_i represents the natural logarithm of corrected detector voltage, x_i is the airmass, and w_i is corrected detector voltage.

APPENDIX C : Alternate Opacity Calculation.(Memorandum dated August 18, 1986)

The Charlottesville radiometer looks at three different temperatures: sky, hot reference, and cold reference. The mathematical expressions for these temperatures are

$$T_s = T_r + (1 - \epsilon)T_1 + \epsilon T_a(1 - e^{-A\tau}) + T_{3K}\epsilon e^{-A\tau} \quad (C - 1)$$

$$T_{cr} = T_r + (1 - \epsilon)T_1 + \epsilon T_c \quad (C - 2)$$

$$T_{hr} = T_r + (1 - \epsilon)T_1 + \epsilon T_h \quad (C - 3)$$

The synchronous detector measures the differences between sky and cold reference and hot and cold reference. The detector outputs for these differences are

$$V_{cs} = \epsilon g(T_a(1 - e^{-A\tau}) + T_{3K}e^{-A\tau} - T_c) + V_{do} \quad (C - 4)$$

$$V_{ch} = \epsilon g(T_h - T_c) + V_{do} \quad (C - 5)$$

where

T_r = receiver temperature

ϵ = coupling efficiency

T_1 = temperature at which losses are terminated

T_a = mean temperature of the atmosphere

τ = atmospheric opacity

A = airmass

T_{3K} = temperature of microwave background radiation

T_c = cold load temperature

T_h = hot load temperature

g = gain constant

V_{do} = detector offset voltage

The detector offset voltage can be removed by taking the difference between equations C - 4 and C - 5.

$$V_{ch} - V_{cs} = G(T_h - T_a(1 - e^{-A\tau}) - T_{3K}e^{-A\tau}) \quad (C - 6)$$

where

$$G = \epsilon g \quad (C - 7).$$

Taking the natural logarithm of equation C - 6 gives

$$\ln(V_{ch} - V_{cs}) = \ln G + \ln((T_h - T_a) + (T_a - T_{3K})e^{-A\tau}) \quad (C - 8)$$

Performing a Taylor's expansion on the second term in the right hand side of equation C - 8, neglecting background radiation, and neglecting terms greater than second order changes C - 8 to

$$\ln(V_{ch} - V_{cs}) = \ln T_h + \ln G - \tau A T_a / T_h + (\tau A T_a / T_h)^2 ((T_h / T_a) - 1) / 2 \quad (C - 9).$$

Equation C - 9 is of the form $y = a + bx + cx^2$ where

$$y = \ln(V_{ch} - V_{cs}) \quad (C - 10)$$

$$x = A \quad (C - 11)$$

$$a = \ln T_h + \ln G = \ln(T_h G) \quad (C - 12)$$

$$b = -\tau T_a / T_h \quad (C - 13)$$

$$c = (\tau T_a / T_h)^2 ((T_h / T_a) - 1) / 2 \quad (C - 14)$$

A nonlinear least squares analysis using $\ln(V_{ch} - V_{cs})$ and A calculates $a, b,$ and c . Since T_h is known, $\tau, T_a,$ and G can be calculated.

$$T_a = T_h / ((2c/b^2) + 1) \quad (C - 15)$$

$$\tau = -T_h b / T_a \quad (C - 16)$$

$$G = e^a / T_h \quad (C - 17)$$

Upon further investigation of this technique, I found that the detector offset voltages in equations C - 4 and C - 5 are not the same. V_{do} in equation C - 4 is the offset voltage for the signal - reference detector circuit. V_{do} in equation C - 5 is the offset voltage for the hot - reference detector circuit. Therefore, taking the difference in equations C - 4 and C - 5 could introduce additional error instead of eliminating the offset voltage. Also, an actual measurement of the offset voltages confirms that they are not zero. The combination of these two facts could account for the instability of this technique.

APPENDIX D : Computer Programs.

1. CVTIPPER
2. SKY
3. DATGRAPH
4. BIGGRAPH
5. CVADJUST
6. SECANT
7. CONSTANT
8. POLYFIT
9. TEMPGRAF

REFERENCES.

1. Bevington, P. R.,1969, **Data Reduction and Error Analysis for the Physical Sciences**, McGraw-Hill, New York.
2. Cota, S. A. and Sramek, R.,1984, **Millimeter Array Memo No.19**.
3. Evans, G. and Mcleish, C. W.,1977, **RF Radiometer Handbook**.
4. Hiltner, W. A.,1962, **Astronomical Techniques**, University of Chicago Press, Chicago.
5. Rybicki, G. B. and Lightman, A. P.,1979, **Radiative Processes in Astrophysics**, John Wiley and Sons, New York.
6. Uson, J. M.,1986, **Millimeter Array Memo No.37**.

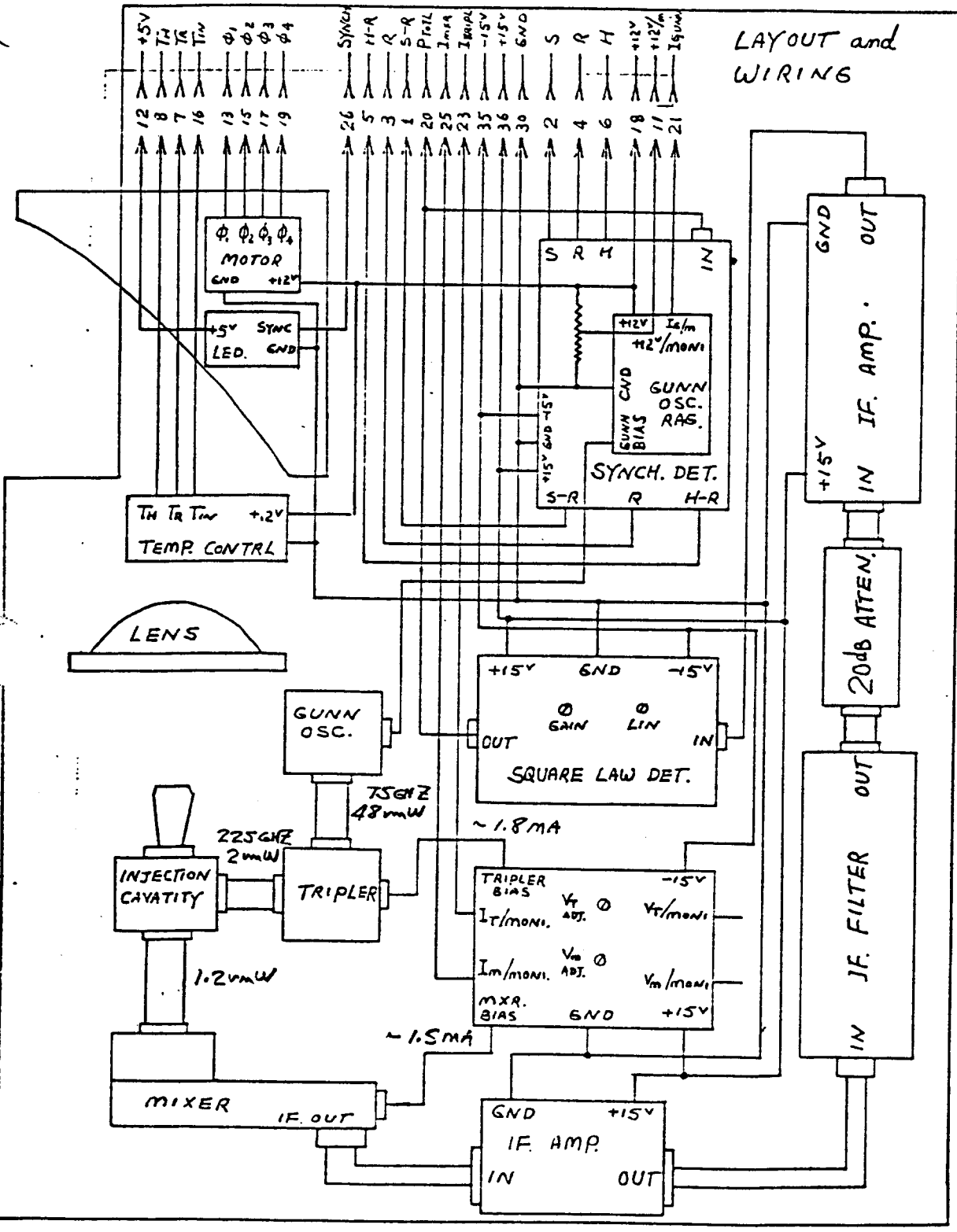


Figure 1: Schematic diagram of Charlottesville 225 GHz radiometer.

Site:VLA
File:b:87012900.dat

Time:2024
Tau = 0.464+/-0.0003
Tat = 258.33+/- 1.21

l
n
V
S
d

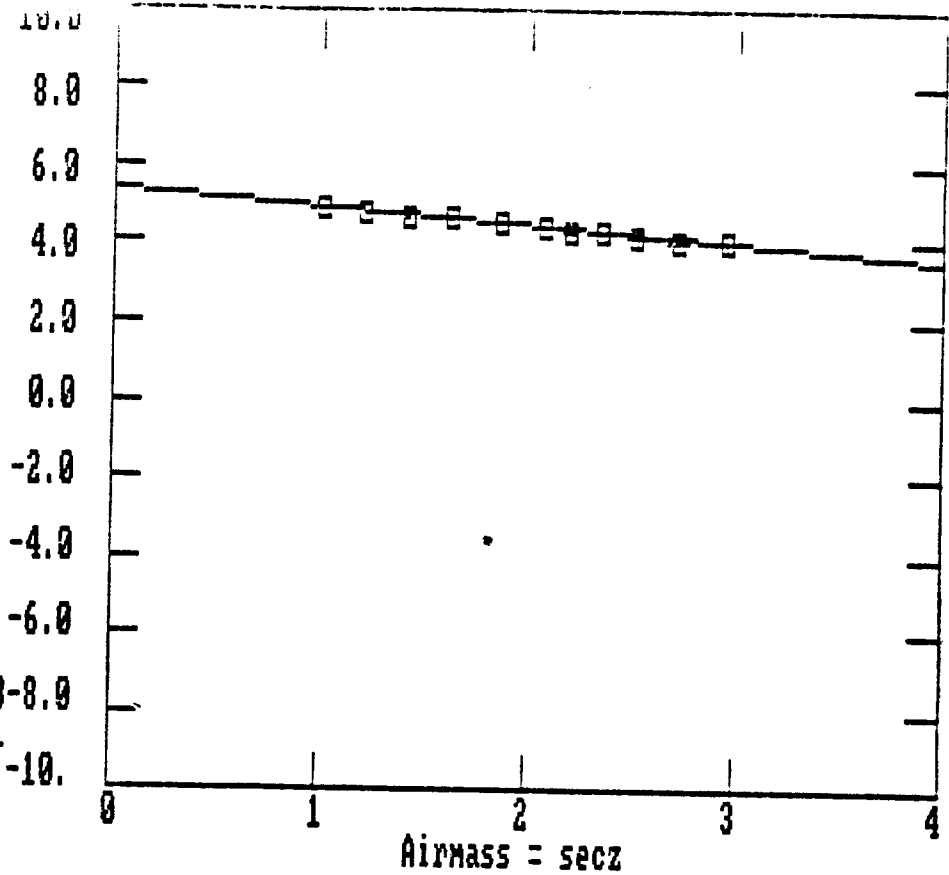
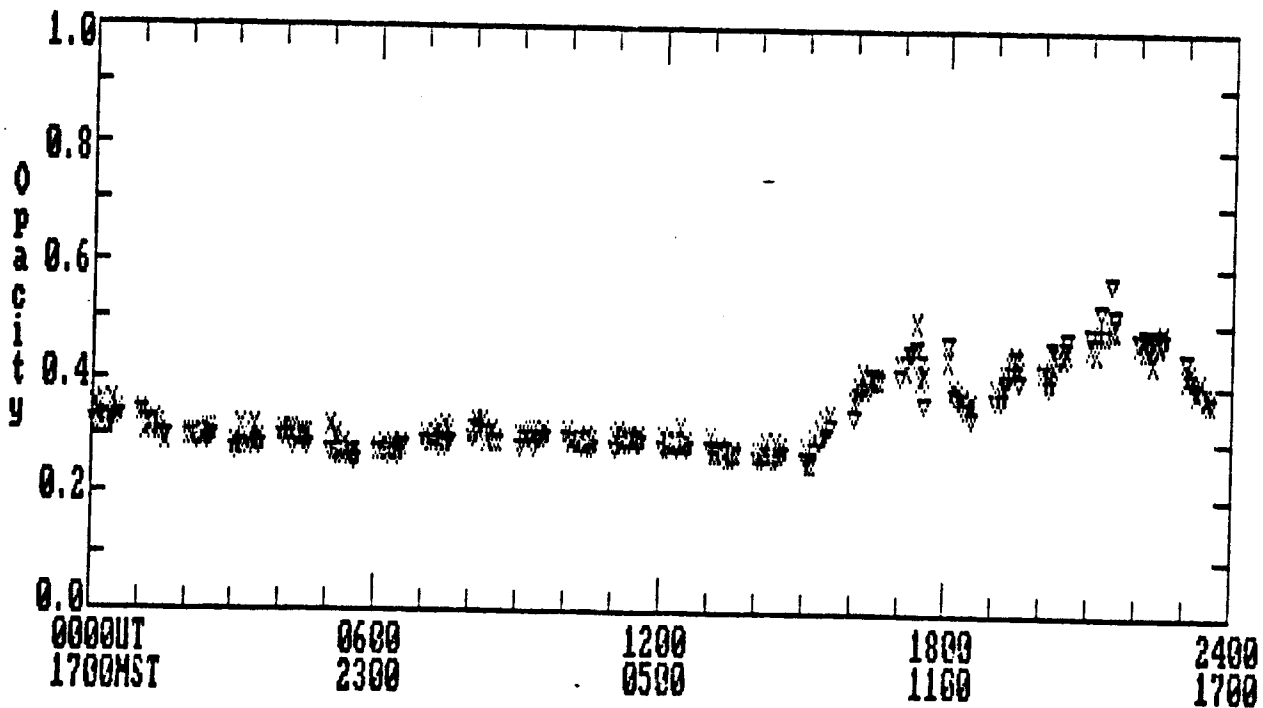


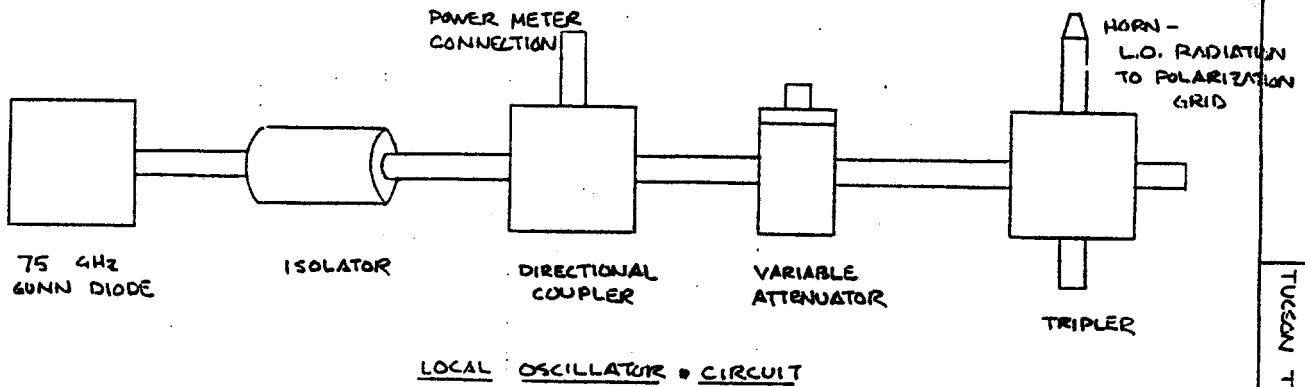
Figure 2: Opacity calculation method for the Charlottesville radiometer. The graph is generated by the program CVADJUST



File: b:87012900.dat
Site: VLA

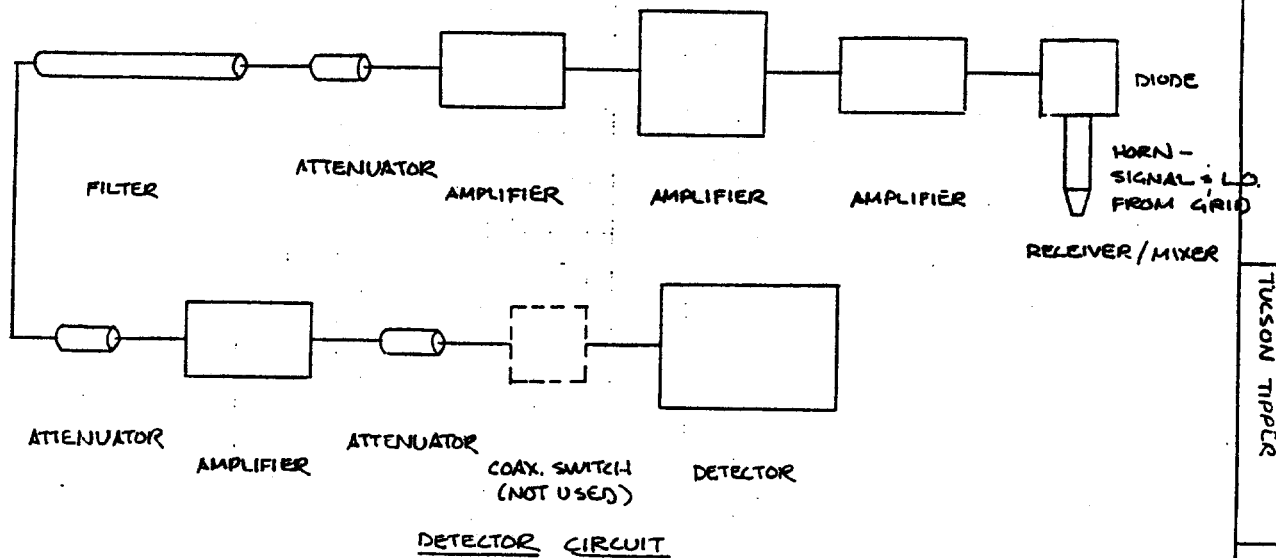
Plot Date: 870130

Figure 3: Scan opacity and zenith opacity as a function of time. The triangles represent scan opacity and the X's represent zenith opacity. The graph is generated by SKY.



1. GUNN DIODE: FREQUENCY SOURCE
2. ISOLATOR: PREVENTS BACKFLOW OF RADIATION POWER (CHECK VALVE)
3. DIRECTIONAL COUPLER: SPLITS SIGNAL - 90%/10%. USED FOR POWER METER CONNECTION.
4. VARIABLE ATTENUATOR: ATTENUATES RADIATION POWER TO DESIRED LEVEL.
5. TRIPLER: MULTIPLIES FREQUENCY BY A FACTOR OF THREE.

Figure 4A: Tucson radiometer local oscillator circuit.



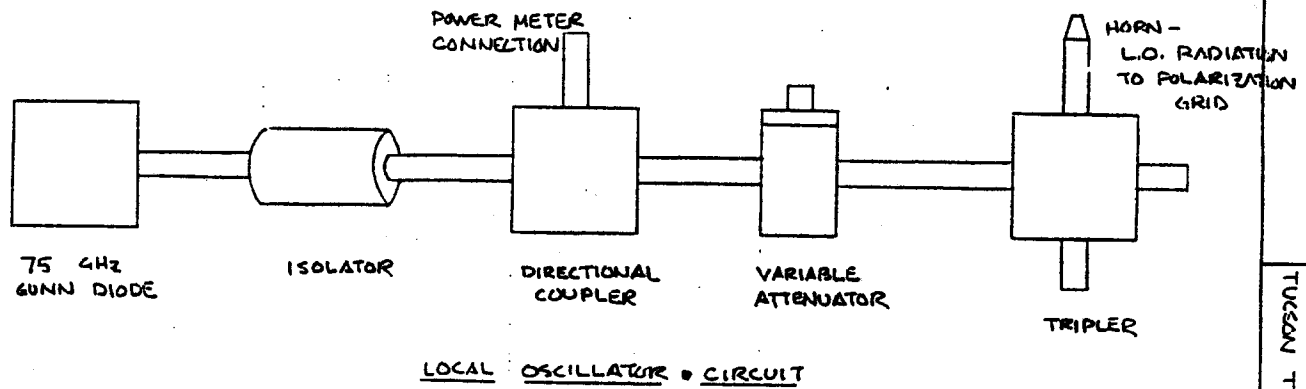
1. RECEIVER/MIXER: RECEIVES COMBINED L.O. & SIGNAL RADIATION, MIXES WITH DIODE.
2. AMPLIFIER: INCREASES RADIATION POWER.
3. ATTENUATOR: DECREASES RADIATION POWER.
4. FILTER:
5. DETECTOR: DETECTS INSTRUMENT SIGNAL & CONVERTS TO ANALOG OUTPUT.

Figure 4B: Tucson radiometer detector circuit.

TUCSON TIPPER

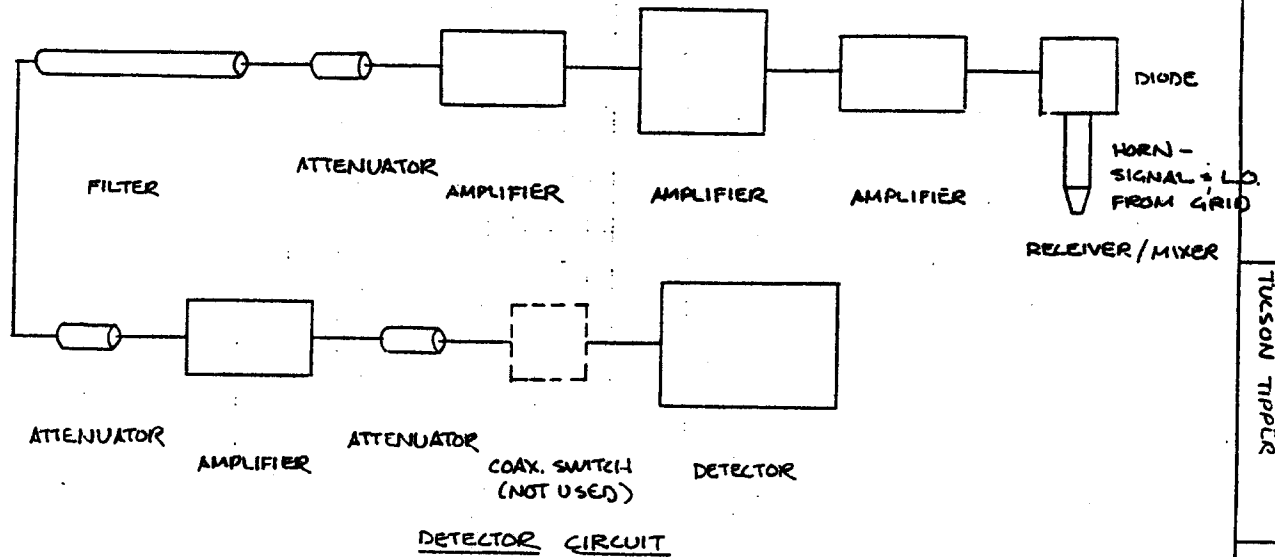
TUCSON TIPPER

MMM - 7/8/86



1. GUNN DIODE : FREQUENCY SOURCE
2. ISOLATOR : PREVENTS BACKFLOW OF RADIATION POWER (CHECK VALVE)
3. DIRECTIONAL COUPLER : SPLITS SIGNAL - 90% / 10%. USED FOR POWER METER CONNECTION.
4. VARIABLE ATTENUATOR : ATTENUATES RADIATION POWER TO DESIRED LEVEL.
5. TRIPLER : MULTIPLIES FREQUENCY BY A FACTOR OF THREE.

Figure 4A: Tucson radiometer local oscillator circuit.



1. RECEIVER/MIXER : RECEIVES COMBINED L.O. & SIGNAL RADIATION, MIXES WITH DIODE.
2. AMPLIFIER : INCREASES RADIATION POWER.
3. ATTENUATOR : DECREASES RADIATION POWER.
4. FILTER :
5. DETECTOR : DETECTS INSTRUMENT SIGNAL & CONVERTS TO ANALOG OUTPUT.

Figure 4B: Tucson radiometer detector circuit.

TUCSON TIPPER

TUCSON TIPPER

MMM - 7/8/86

File:86061800.dat
Time:2323
Tau = 0.559
Fit = -0.981

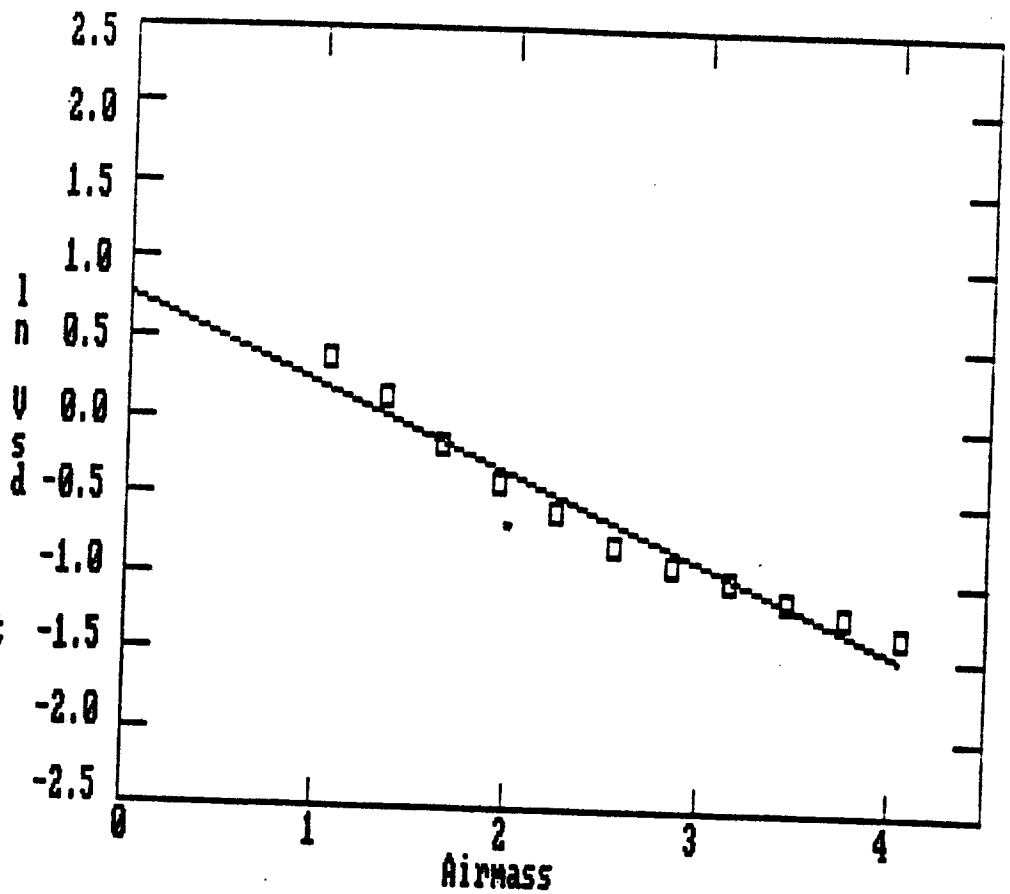


Figure 5: Original opacity calculation method for the Tucson radiometer. The graph is generated by the program BIGGRAPH.

File:86061000.dat
Time:2323
a = 1.522
b = -1.235
c = 0.132

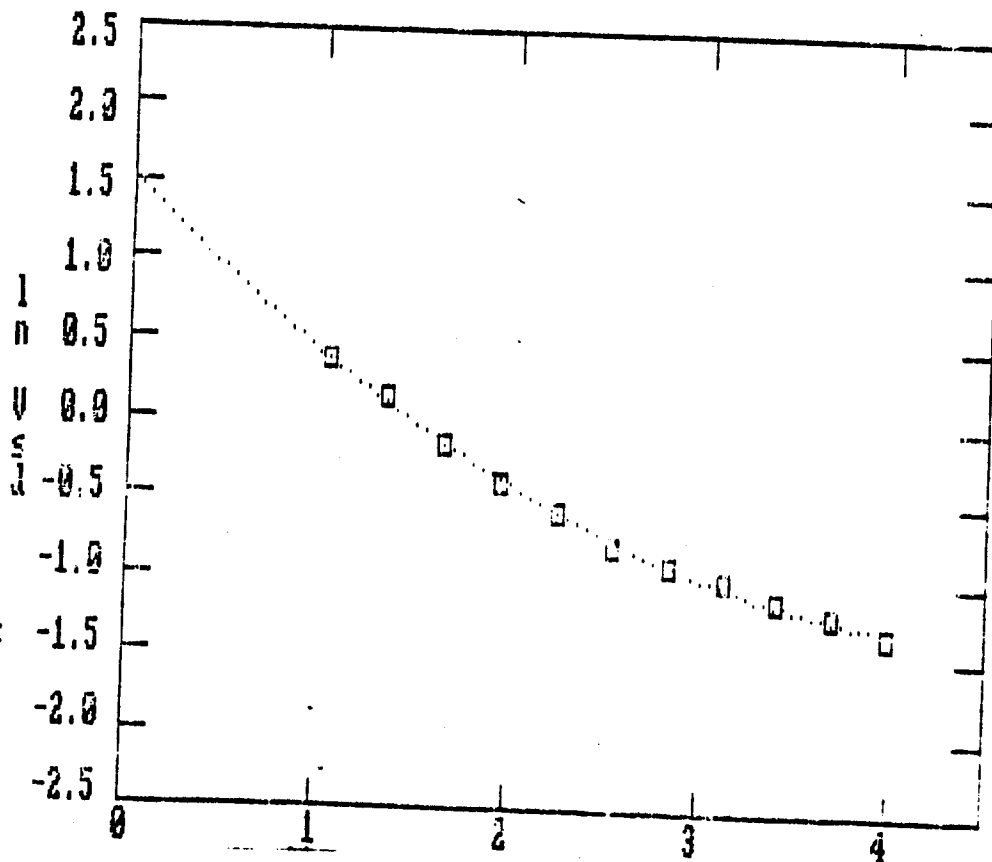


Figure 6: Quadratic opacity calculation method for the Tucson radiometer. The graph is generated by the program POLYFIT.

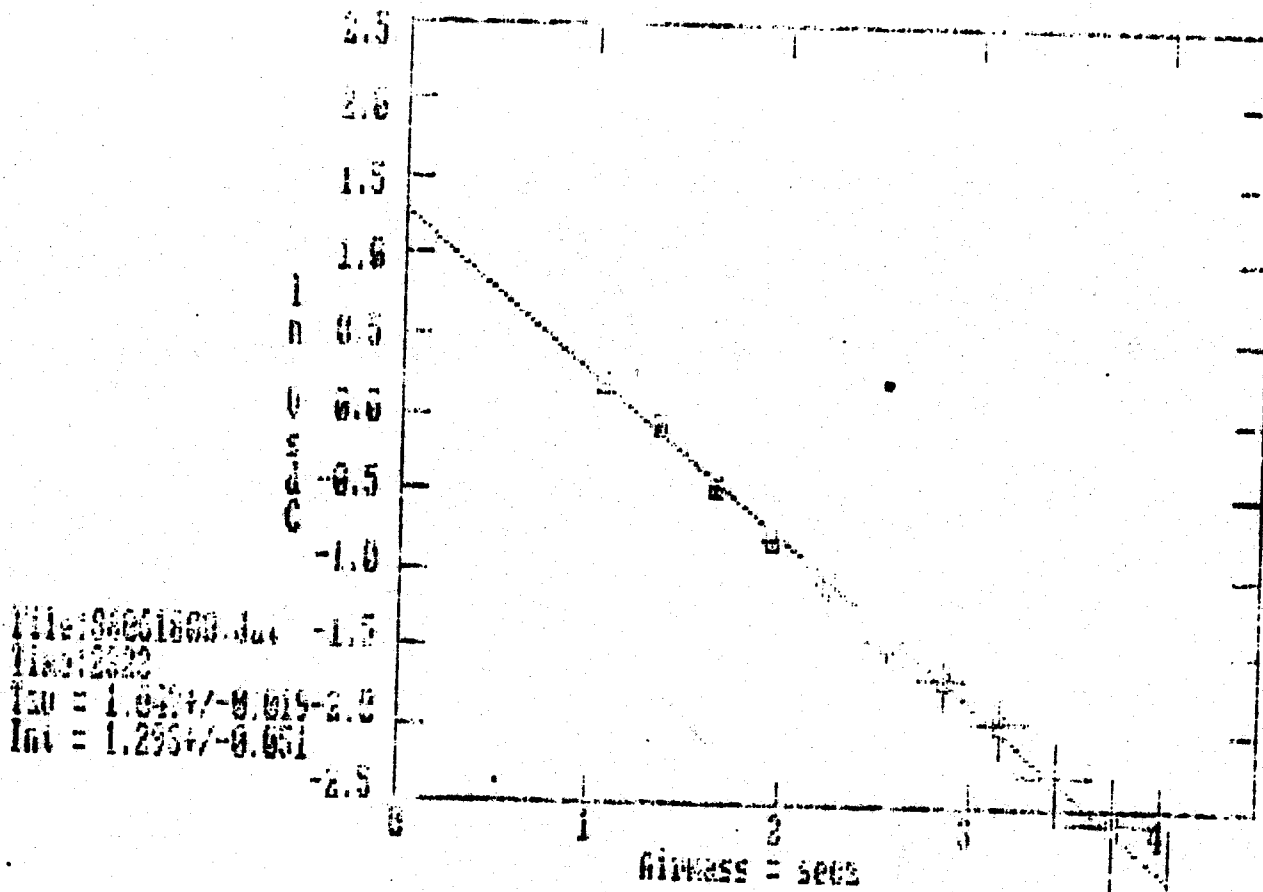
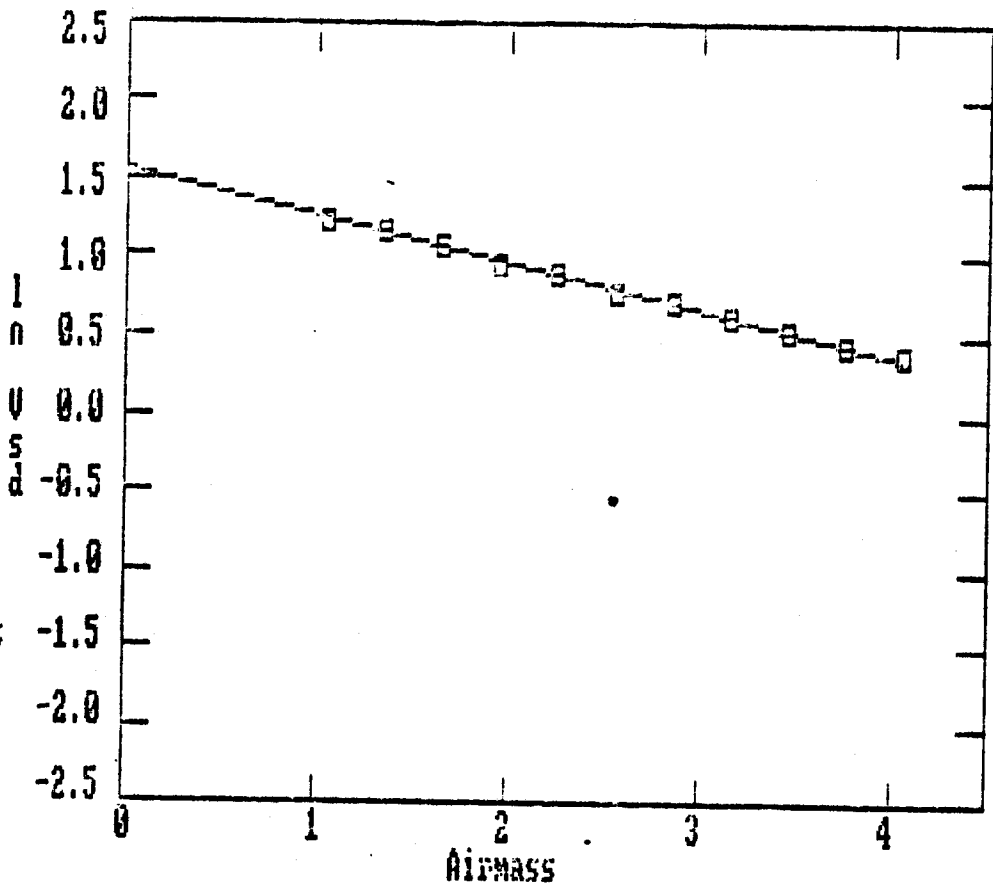
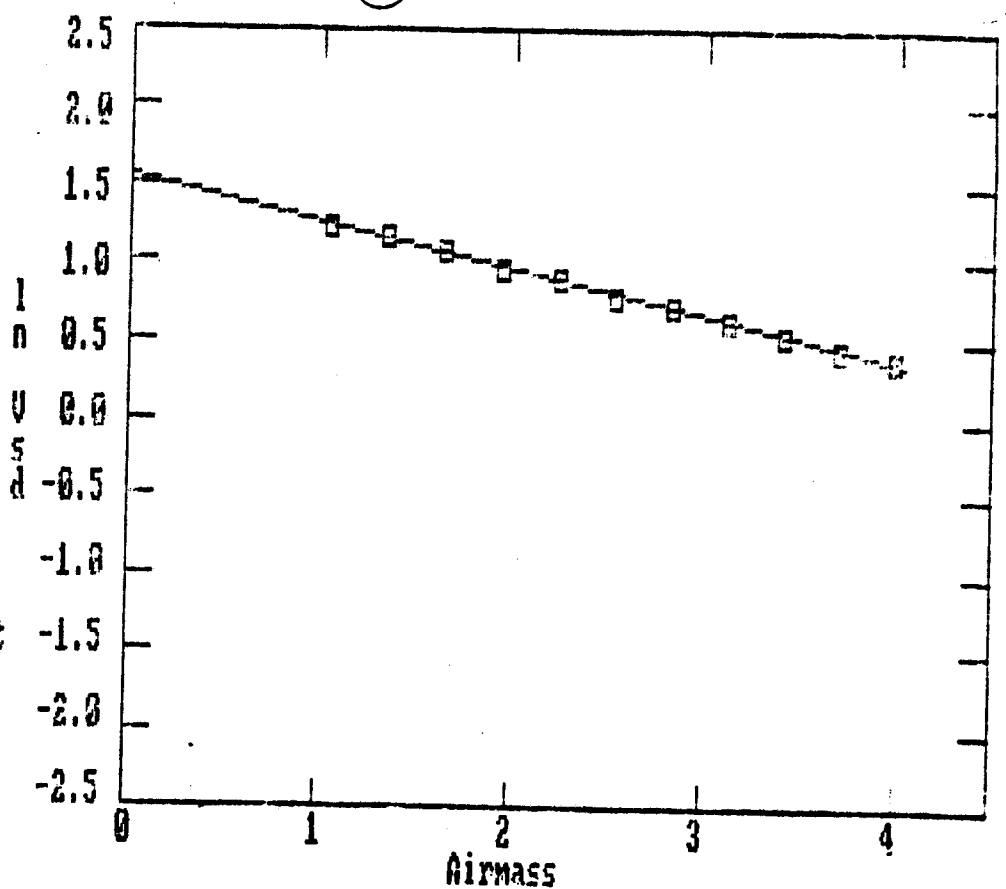


Figure 7: Opacity calculation method which assumes atmosphere temperature is 95 percent of ambient temperature. Note the difference in airmass uncertainty between three and four airmasses. The graph is generated by the program CONSTANT.



File:86062100.dat
 Time:1633
 Tau = 0.293
 Fit = -0.998

Figure 8A: Airmass determined by sec(z). The graph is generated by the program BIGGRAPH.



File:86062100.dat
 Time:1633
 Tau = 0.298
 Fit = -0.998

Figure 8B: Airmass determined by equation $V - 1$. The graph is generated by the program SECANT.

ZENITH ANGLE = -34.2

#	ITEM	mVOLTS	SCALED
0)	SIG-REF	-4910.31	-245.516K
1)	HOT-REF	3729.69	18.648K
2)	REF	-3895.31	3052.344K
3)	REF TEMP	4459.69	44.597C
4)	HOT TEMP	6484.69	64.847C
5)	OUT TEMP	2719.69	27.197C
6)	IN TEMP	4659.69	46.597C*
7)	MXR CUR	-2100.31	2.100mA
8)	TRIP CUR	-1355.31	1.355mA
9)	GUNN CUR	1959.69	0.196A
10)	SUP VOLTS	5914.69	11.829V
11)	ZEN ANG	-2280.31	-45.606deg
12)	SUP CUR	3984.69	3.985A
13)	SPARE 2	2534.69	2534.687
14)	SPARE 3	-1245.31	-1245.312
15)	SPARE 4	-5500.31	-5500.312

Figure 9A: Output of the program CVTIPPER during a tipping scan.

370620 1834UT TAU = 0.184 +/- 0.0002
tauz = 0.208
Airmass: 1.01 1.21 1.41 1.63 1.87 2.08 2.20 2.35 2.52 2.72 2.95
ln(vsd): 5.47 5.44 5.42 5.38 5.34 5.30 5.28 5.26 5.23 5.21 5.18
rms(vsd): 0.34 0.28 0.42 0.22 0.28 0.25 0.29 0.28 0.15 0.25 0.24

minutes = 1115 Next Tau scan at 1120

Figure 9B: Output of the program CVTIPPER after a tipping scan.

MMIA

7-8-56

ELECTRICAL SCHEMATIC -
TIPPER TIME DELAY RELAY

1/2

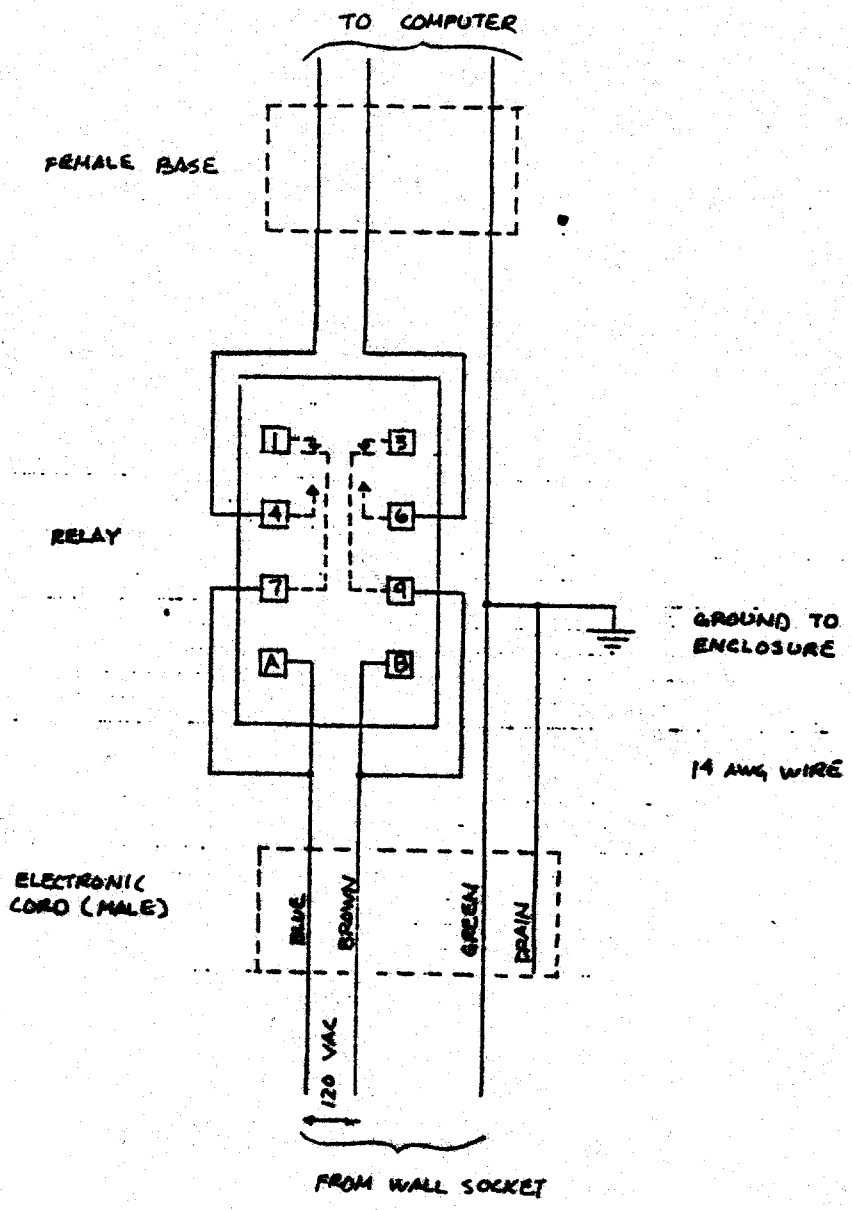


Figure 13: Time delay relay circuit drawing.

LV RADIONETER SUPPORT
 (SCALE: 1 1/2" = 1'-0")
 MMN - 9-19-86

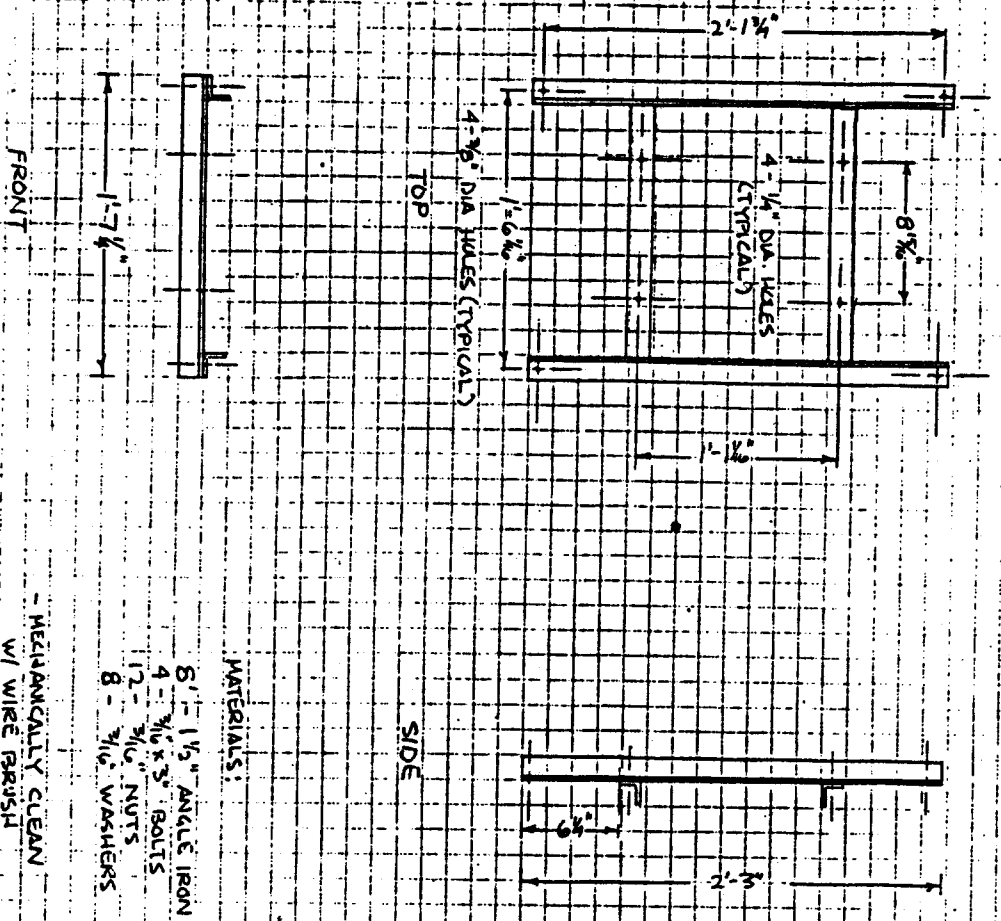


Figure 12C: Modification to support stand for Charlottesville radiometer installation.

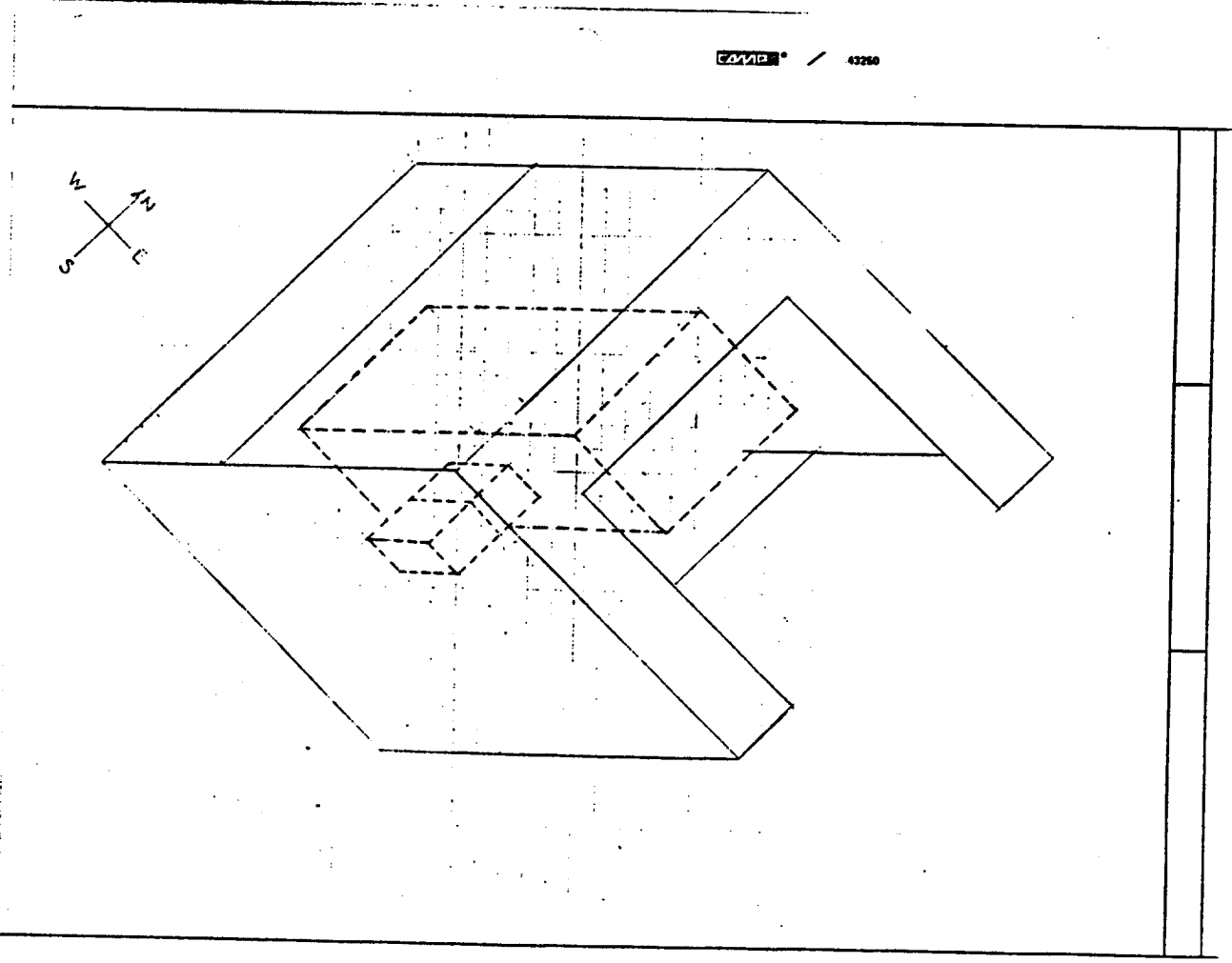
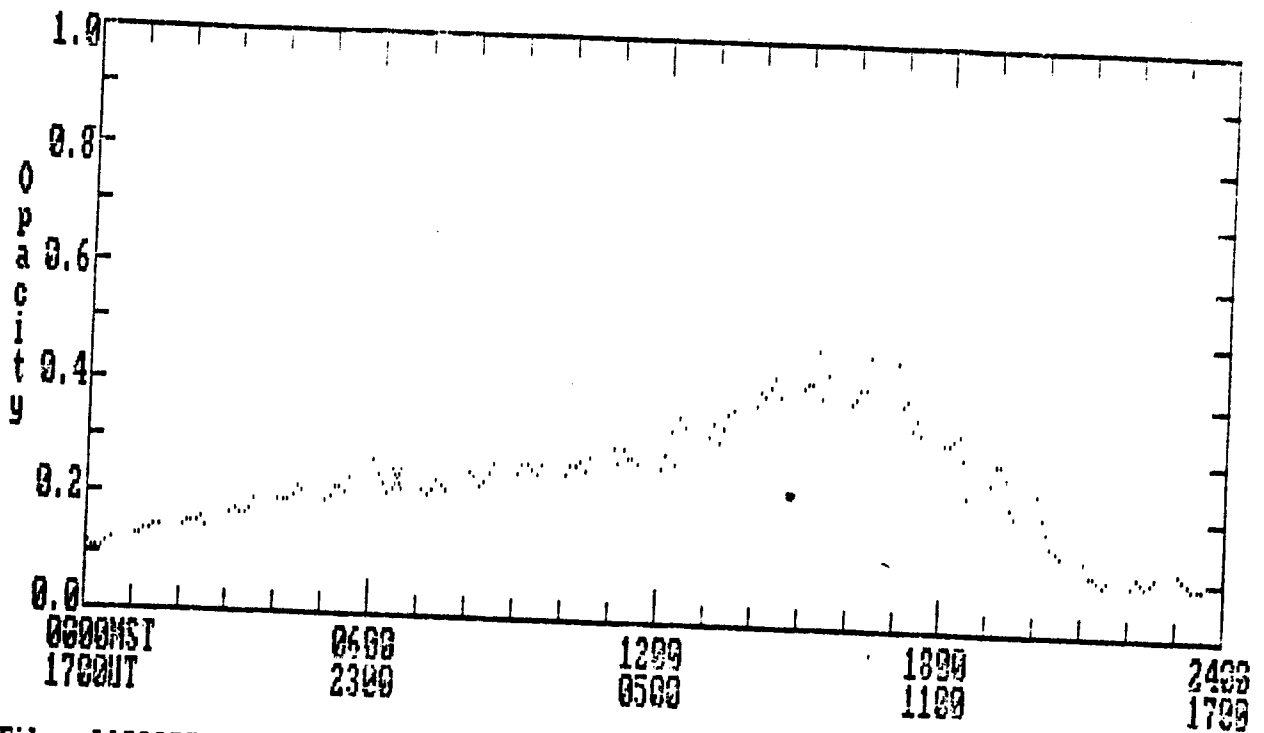


Figure 12D: Isometric view of Charlottesville radiometer enclosure.

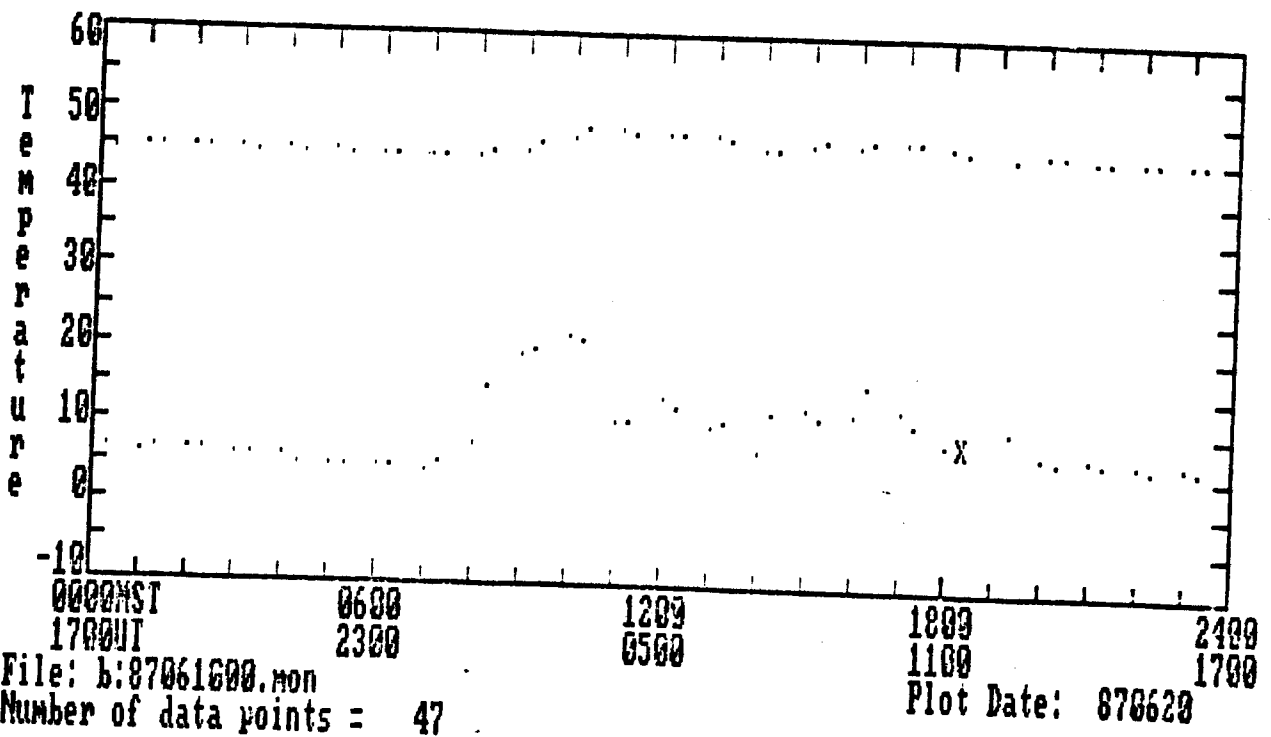


File: 86022700.dat

Number of data points = 144

Plot Date: 860709

Figure 10: Night-day variations in opacity as measured by the Tucson radiometer. The graph is generated by the program DATGRAPH.



File: b:87061600.mon

Number of data points = 47

Plot Date: 870620

Figure 11: Variation in Charlottesville radiometer enclosure temperature with ambient temperature. The upper row of dots represents the enclosure temperature which is controlled at 45C. The lower set of dots represents ambient temperature.

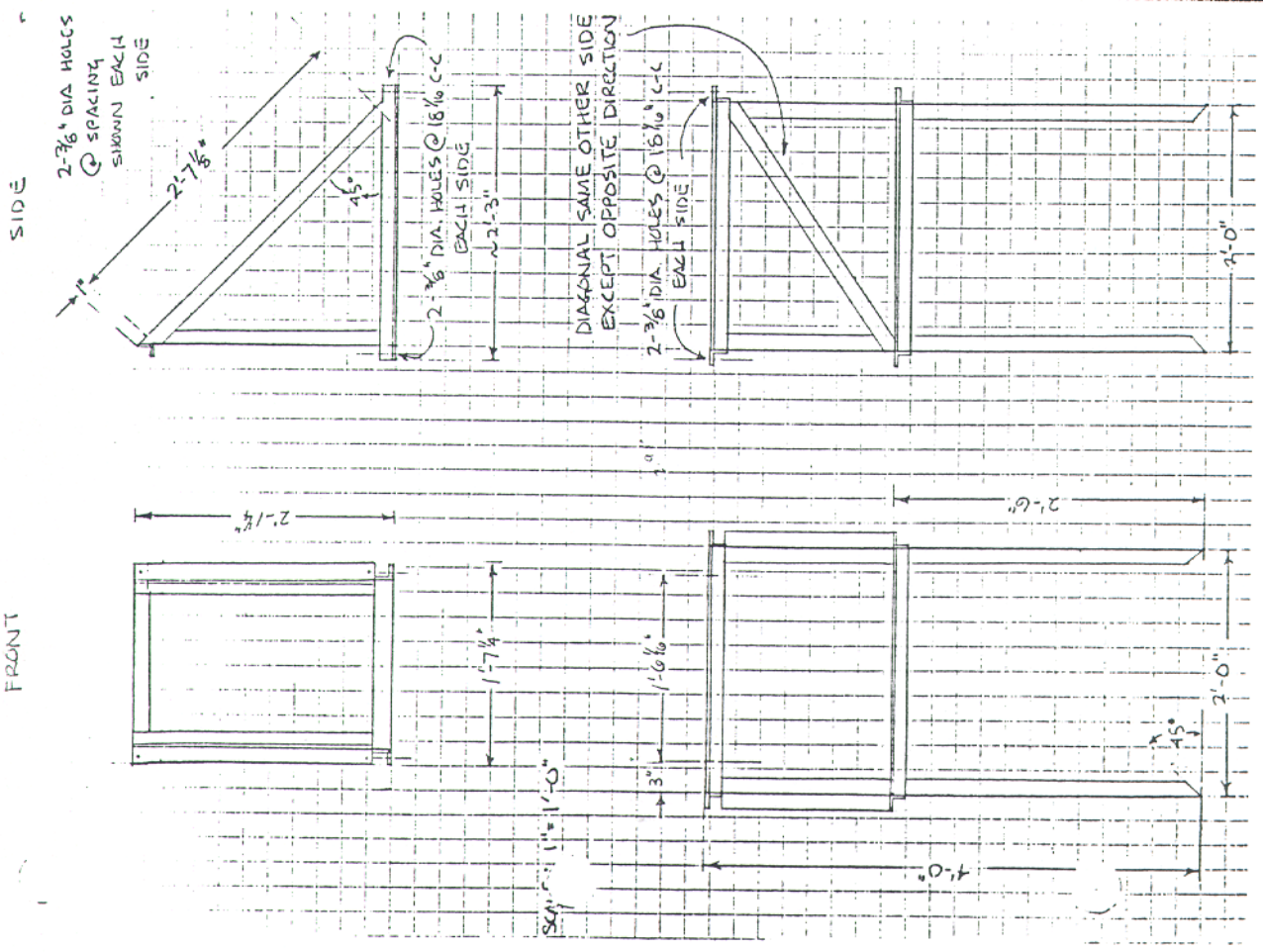
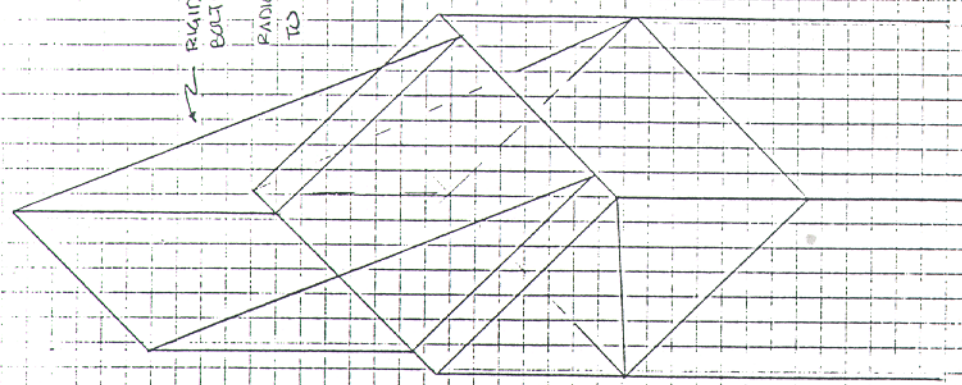


Figure 12A: Plan view of Tucson radiometer support stand.

- MATERIALS:**
- 60' - 1 $\frac{1}{2}$ " ANGLE IR
 - 8 - 1 $\frac{1}{4}$ " x 1" BOLTS w/ WASHERS (M)
 - Mechanically Clean
 - w/ WIRE BRUSH
 - ONE COAT PRIMER
 - TWO COATS FINISH (WHITE)



RAISE UPPER STRUCTURE BOLTS TO LOWER STRUCTURE

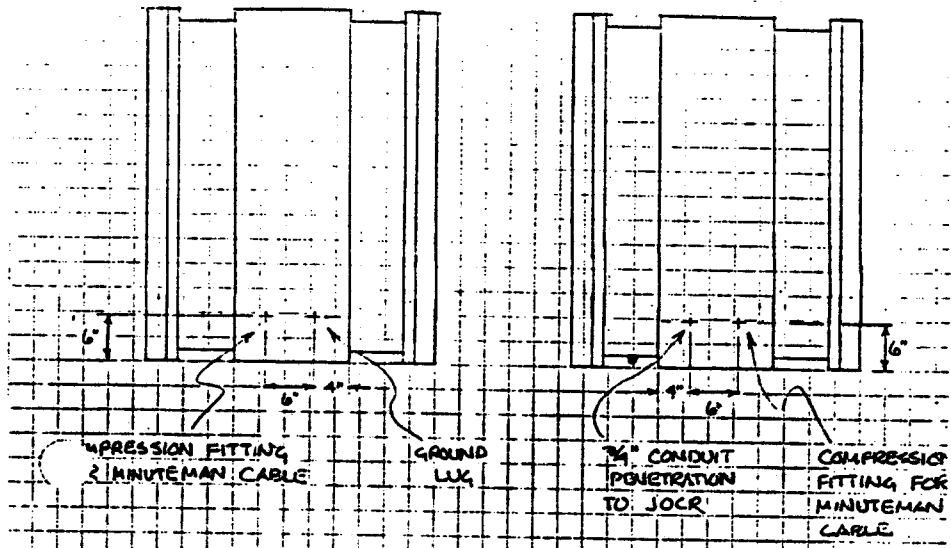
RADIOMETER ENCLOSURE BOLTS TO UPPER STRUCTURE

Figure 12B: Isometric view of Tucson radiometer support stand.

SOUTH SIDE
(TO LANG. LAB.)

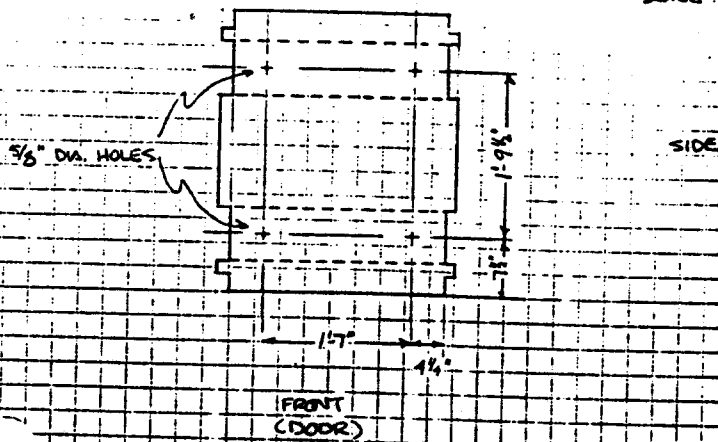
NORTH SIDE
(TO KIVA)

SCALE: 3/4" = 1'-0"



BOTTOM VIEW
(ANCHOR BOLT LOCATION)

SCALE: 3/4" = 1'-0"



BILL OF MATERIAL
JUNCTION BOX MODIFICATIONS

CONSTRUCTION
SUGGESTIONS

- 2- COMPRESSION FITTINGS
- 2- TERMINAL STRIPS W/ MOUNTING SCREWS
- 1- 3/4" CONDUIT PENETRATION FITTING
- 1- GROUND LUG
- GASKET MATERIAL
- 1- GROUND ROD
- GROUND WIRE

GASKET PENETRATIONS
TO PREVENT WATER
SEEPAGE

Figure 14A: Junction box modification.

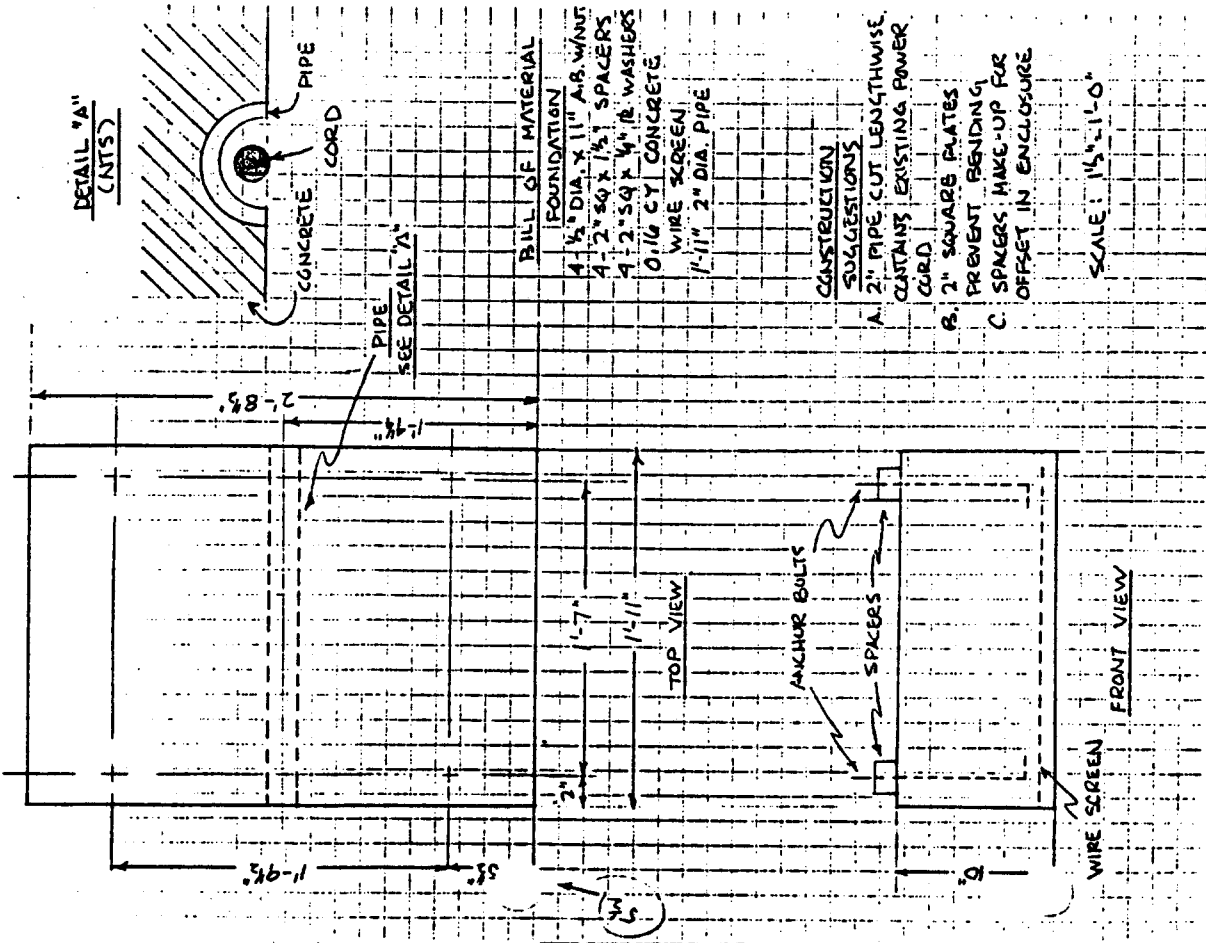


Figure 14B: Junction box foundation.

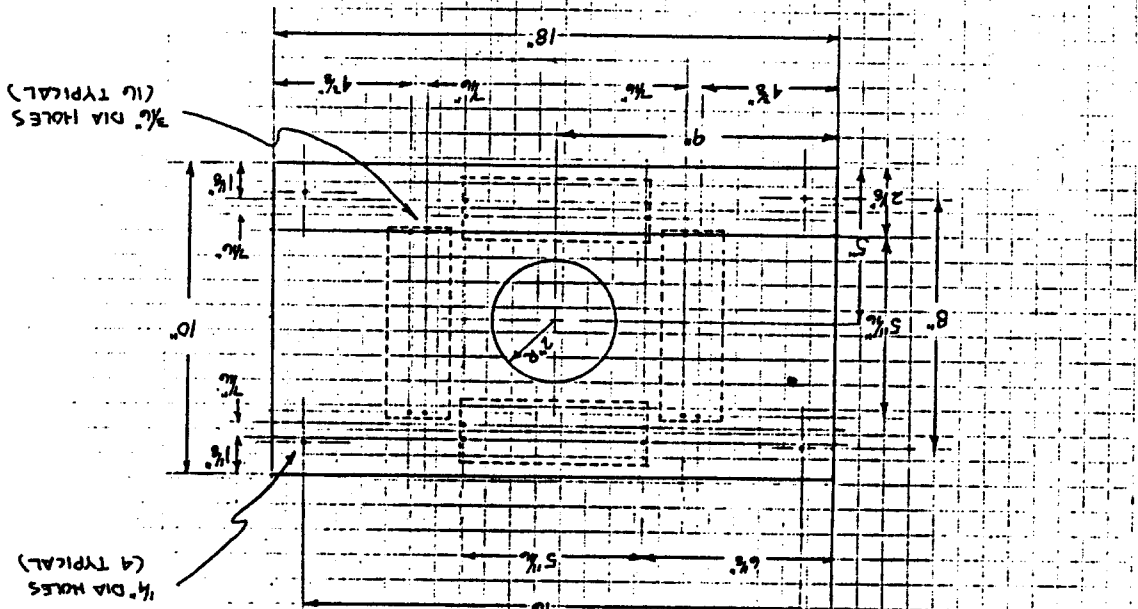


Figure 14C: Terminal strip installation.

SOUTH BALDY DATA

86NOV08-87MAR31

NO. POINTS

3456

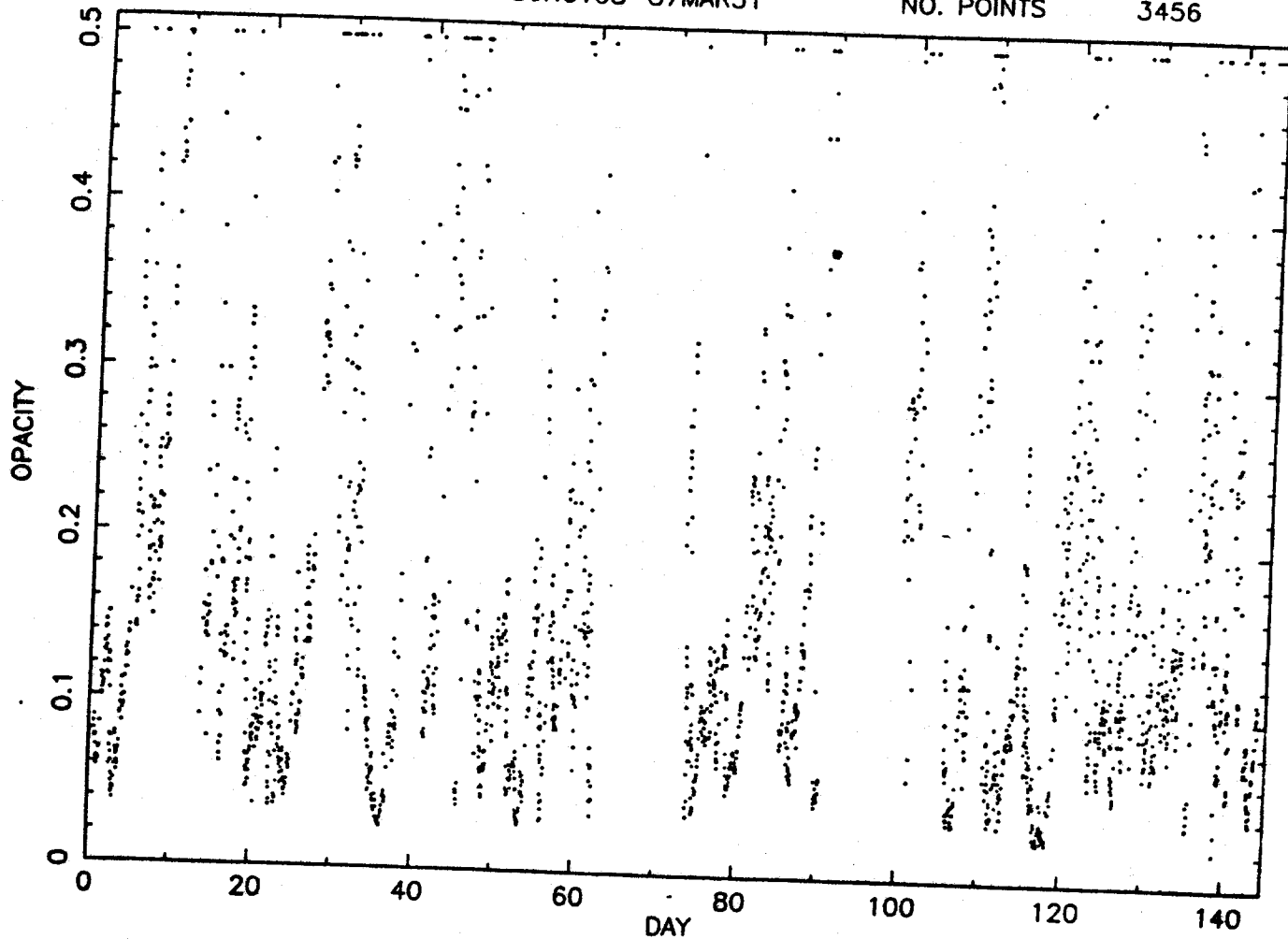


Figure 15: Opacity at South Baldy.

VLA SITE DATA

86DEC30-87FEB28

NO. POINTS

1457

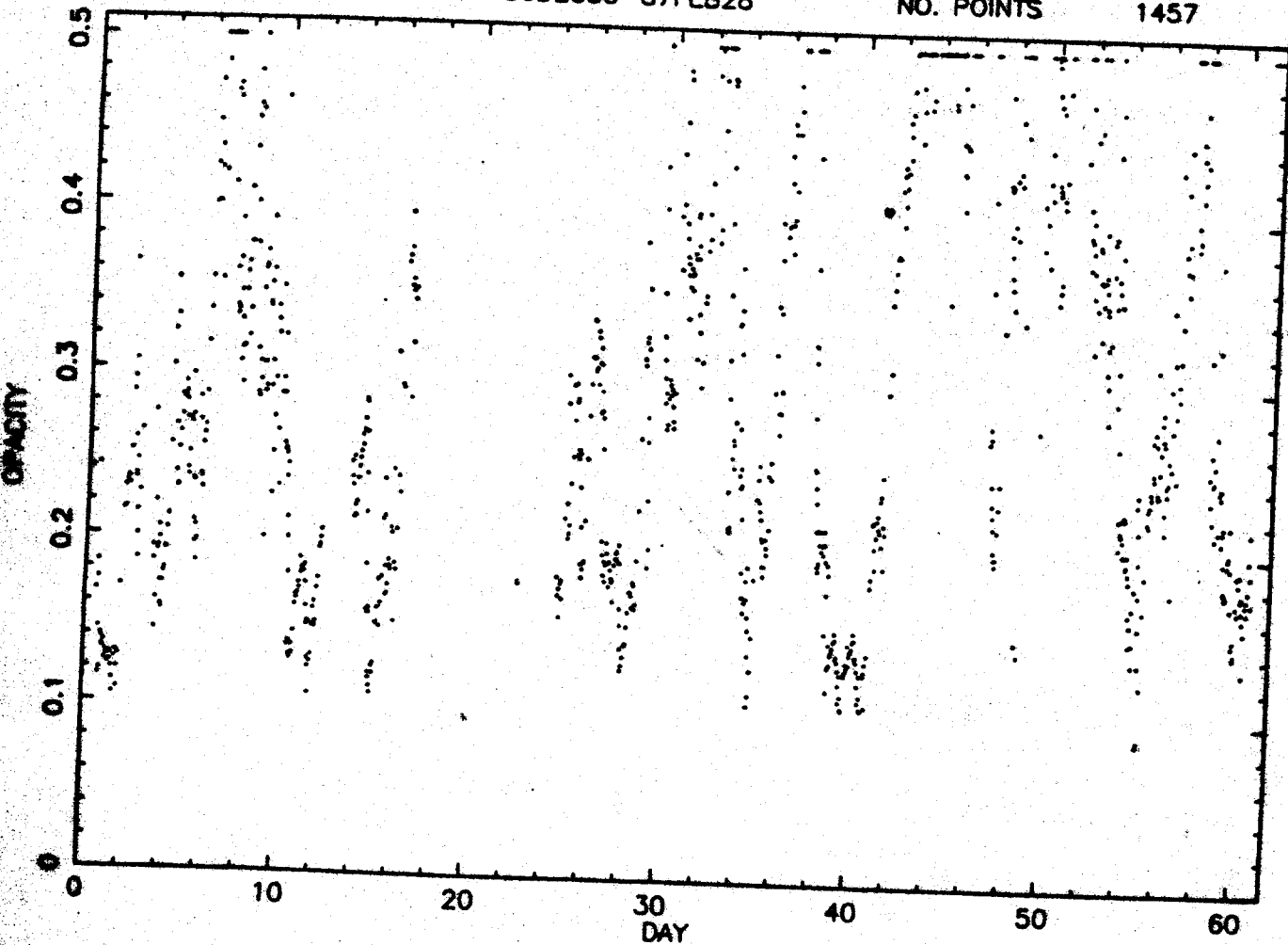


Figure 16: Opacity at the VLA.